

Design and Performance of Dual-Hop MIMO UWB Transmissions

Kiattisak Maichalernnukul, *Student Member, IEEE*, Feng Zheng, *Senior Member, IEEE*, and Thomas Kaiser, *Senior Member, IEEE*

Abstract—To coexist with existing legacy wireless systems, the transmit power spectral density of ultrawideband (UWB) impulse radio systems is limited. The coverage range of UWB systems is then confined to within a few meters. Dual-hop relaying or multiple-input–multiple-output (MIMO) technology is one possible way of achieving greater UWB system coverage. This paper presents the design of dual-hop UWB MIMO relay systems (in which a source, relay, and destination have multiple antennas) according to the availability of channel state information (CSI) and their performance analysis over a UWB multipath fading channel. In particular, the decouple-and-forward and decode-and-forward relay systems are proposed when partial CSI is only available at the receiver side. On the other hand, with partial CSI being available at the transmitter side, we propose the amplify-and-forward and detect-and-forward relay systems. The exact formulas for the outage probabilities of those systems are derived. Furthermore, we evaluate, in closed form, the amount of fading and bit error rate expressions under sufficiently high signal-to-noise ratio and verify them through comparison with the simulation results. The effect of spatial correlation on the performance of our proposed systems is also studied. Numerical examples of the results provide valuable insights into the design of UWB MIMO relay systems.

Index Terms—Amount of fading (AOF), bit error rate (BER), multiple-input–multiple-output (MIMO), outage probability, relay system, ultrawideband (UWB).

I. INTRODUCTION

ULTRAWIDEBAND (UWB) impulse radio has gained much interest because of its potential to deliver high data rates over short distances and to overlay spectrum with licensed narrowband radios [1]–[3]. UWB impulse radio systems utilize extremely wide frequency bands where various legacy narrowband systems operate; therefore, their transmit power spectral density (PSD) is restricted according to Federal Communications Commission (FCC) regulations [4], which leads to limited system coverage. One viable approach to overcoming this limitation is to employ relays as used in conventional cellular systems [5]. More precisely, the relays allow for a reduction of the end-to-end path loss between a data source and its destination and, as a result, could extend the coverage without using more power at the source.

Manuscript received October 11, 2009; revised February 9, 2010 and March 26, 2010; accepted March 28, 2010. Date of publication April 15, 2010; date of current version July 16, 2010. The review of this paper was coordinated by Dr. C. Ling.

The authors are with the Institute of Communications Technology, Faculty of Electrical Engineering and Computer Science, University of Hannover, 30167 Hannover, Germany (e-mail: kiattisak.maichalernnukul@ikt.uni-hannover.de; feng.zheng@ikt.uni-hannover.de; thomas.kaiser@ikt.uni-hannover.de).

Color versions of one or more of the figures in this paper are available online at <http://ieeexplore.ieee.org>.

Digital Object Identifier 10.1109/TVT.2010.2048347

In general, the relays can be classified as either amplify-and-forward (AF) or decode-and-forward (DF) relays. Recently, their potential to extend the coverage of the UWB impulse radio systems or improve their reliability has been demonstrated by many researchers [6]–[12].¹ While the work in [6]–[10] is built on the assumption that each relay is equipped with a single antenna, we provided the performance analysis of dual-hop UWB relay systems with a two-antenna DF relay in [11] to illustrate the benefits of multiple-antenna deployment at the relay. In [12], we introduced a dual-hop UWB relay system using multiple DF relays, each of which is equipped with multiple antennas, and showed that increasing the number of antennas at each relay can generally gain more performance improvement than increasing the number of relays. Thus, it might be preferable to utilize a few relays with more antennas for common UWB relay systems if the space at the relays is available as in fixed relay networks, see, e.g., [17].

Motivated by multiple-input–multiple-output (MIMO) performance enhancement in point-to-point communication systems [18], [19], there has been great interest in narrowband MIMO relay systems where the source, relay(s), and destination have multiple antennas [20]–[24]. The design and/or performance of these systems that operate under different fading conditions have been well studied; see, e.g., [22]–[24]. However, such treatment has not explicitly been provided, so far, for UWB MIMO relay systems, although the potential benefits of UWB systems combined with MIMO techniques have been shown in recent studies for UWB nonrelay systems; see [25] and the references therein.

The main objective of this paper is to present the design and performance analysis of UWB MIMO relay systems. Based on the availability of channel state information (CSI), we design two kinds of such systems, i.e., *receiver-CSI-assisted* and *transmitter-CSI-assisted relay systems*, where partial CSI is available only at the receiver side and only at the transmitter side, respectively, and the corresponding relaying schemes.² Through theoretical analysis and simulations, the system performance subject to a UWB frequency-selective channel is analyzed in terms of outage probability, amount of fading (AOF), and bit error rate (BER). Because spatial correlation in UWB

¹See [13]–[16] for this aspect in the narrowband context.

²Although the main ideas of the relaying schemes in this paper already exist in narrowband relay systems, the unique properties of UWB systems, such as high multipath resolution (which implies a large number of resolvable paths) and carrierless transmission [1], make the detailed design and analyzed performance of the aforementioned UWB relay systems significantly different from that of their narrowband counterparts.

channels is a critical factor that affects the performance of UWB MIMO nonrelay systems [25], [26], we also quantify the effect of such correlation on the performance of the designed relay systems. Numerical results based on both theoretical analysis and simulations provide basic guidelines for the design of the UWB MIMO relay systems, e.g., the appropriate use of transmit and/or receive antennas for different kinds of relay systems.

The rest of this paper is organized as follows. In Section II, the UWB channel model and the UWB MIMO relay system model are described. Sections III and IV present the receiver-CSI-assisted and transmitter-CSI-assisted relay systems, respectively, both with their performance analysis. Section V provides the numerical results of theoretical analysis and simulations, and Section VI concludes the paper.

Notation

Bold uppercase letters denote matrices, and bold lowercase letters denote column vectors. \mathbf{I}_N is the identity matrix of size $N \times N$. $\mathbf{1}_N$ is the all-ones column vector of length N . $[\cdot]_{ij}$, $[\cdot]_r$, $(\cdot)^\dagger$, $\|\cdot\|^2$, and $\det(\cdot)$ denote the (i, j) th element, r th row, transpose, squared Frobenius norm, and determinant of a matrix, respectively. \otimes denotes the Kronecker product, and $*$ denotes the convolution. $|\cdot|$ and $\text{sign}(\cdot)$ denote the absolute value and sign operator, respectively. We use the notations $f_X(x; a, b)$ and $F_X(x; a, b)$ to refer to the probability density function (pdf) and cumulative density function (cdf) of the random variable X , possibly with parameters a and b , respectively. $\mathcal{M}_X(s) = \text{E}[\exp(sX)]$ denotes the moment-generating function (MGF) of X , where $\text{E}[\cdot]$ denotes the expectation operator. $(\partial^n / \partial s^n)(\cdot)$ denotes the n th partial derivative operator with respect to the variable s . Subscripts S, R, and D denote the source, relay, and destination in a relay system, respectively. $U(\cdot)$, $\Gamma(\cdot, \cdot)$, $\Gamma(\cdot)$, $\mathcal{K}_n(\cdot)$, ${}_2F_1(\cdot, \cdot; \cdot; \cdot)$, $Q(\cdot)$, and $\text{erfc}(\cdot)$ denote the Heaviside step function, upper incomplete gamma function, ordinary gamma function, n th-order modified Bessel function of the second kind, Gauss hypergeometric function, Gaussian Q -function, and complementary error function defined in [27, eq. (17.13.93)], [27, eq. (8.350.2)], [27, eq. (8.310.1)], [27, eq. (8.432)], [27, eq. (9.100)], [28, eq. (4.1)], and [27, p. xxxvii], respectively. $\binom{\cdot}{\cdot}$ is the binomial coefficient defined in [27, p. xlv].

II. CHANNEL AND SYSTEM MODELS

In general, a UWB link channel can be modeled by the stochastic tapped-delay-line propagation model [25], [29]–[31]. Accordingly, the channel impulse response (CIR) for a UWB transmission link can be described by³

$$h(t) = \sum_{l=0}^{L_t-1} \alpha_l \delta(t - lT_w) = \sqrt{P} \sum_{l=0}^{L_t-1} \varphi_l \delta(t - lT_w) \quad (1)$$

³In the literature on UWB channel models, both dense and sparse multipath channels exist. In a dense channel, e.g., as observed in office and industrial environments [29], [32], each resolvable delay bin contains significant energy, and a tapped-delay-line model with regularly spaced arrival times of resolvable multipath components gives a good approximation for the exact channel model. In some other environments, e.g., [33], a sparse channel has been observed, i.e., not every resolvable bin contains energy, and the arrival times are described as a continuous-time stochastic point process. For analytical convenience, we consider only the former case.

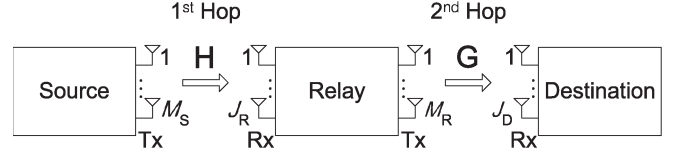


Fig. 1. System model.

where L_t is the number of multipath components, l is the path index, α_l is the l th path channel coefficient, T_w is the minimum multipath resolution, φ_l is the energy-normalized channel coefficient with $\text{E}[\sum_{l=0}^{L_t-1} \varphi_l^2] = 1$, and P is the total multipath gain. The minimum multipath resolution T_w is equal to the width of the unit-energy monocycle pulse $w(t)$, because any two paths whose relative delay is less than the pulse width are not resolvable. The gain P is the reciprocal of the path loss that is modeled as a function of the link distance and given in [29, eq. (1)]. Let us denote φ_l as $\varphi_l = \theta_l v_l$, where $\theta_l = \text{sign}(\varphi_l)$ and $v_l = |\varphi_l|$. The variable θ_l takes the signs $+1$ and -1 with equal probability to account for the signal inversion due to reflection. The variable v_l follows the Nakagami- m distribution [25], [29], with the pdf given by

$$f_{v_l}(x; m, \eta_l) = \frac{2x^{2m-1}}{\eta_l^m (m-1)!} \exp\left(-\frac{x^2}{\eta_l}\right) U(x) \quad (2)$$

where $\eta_l = \Omega_l / m$, and $\Omega_l = \text{E}[v_l^2]$ exponentially decreases with the excess delay, i.e., $\Omega_l = \varpi \Omega_{l-1}$ where $\varpi < 1$ is a constant. The value of ϖ is determined by the communication scenario. Throughout this paper, we assume that m is an integer and is fixed for all the path indexes. The first assumption on m is necessary for the theoretical analysis hereafter, whereas the second assumption is for analytical convenience. Define $\chi_l = \varphi_l^2 = v_l^2$. Hence, χ_l follows the Gamma distribution whose pdf and cdf, respectively, are

$$\begin{aligned} f_{\chi_l}(x; m, \eta_l) &= \frac{x^{m-1}}{\eta_l^m (m-1)!} \exp\left(-\frac{x}{\eta_l}\right) U(x) \quad (3) \\ F_{\chi_l}(x; m, \eta_l) &= \left[1 - \frac{\Gamma\left(m, \frac{x}{\eta_l}\right)}{(m-1)!} \right] U(x) \\ &= \left[1 - \exp\left(-\frac{x}{\eta_l}\right) \sum_{k=0}^{m-1} \frac{1}{k!} \left(\frac{x}{\eta_l}\right)^k \right] U(x). \quad (4) \end{aligned}$$

We consider the dual-hop relayed UWB transmission system in Fig. 1. Here, the source that is equipped with M_S transmit antennas communicates with the destination that is equipped with J_D receive antennas through an intermediate relay. The relay consists of J_R receive and M_R transmit antennas. Let \mathbf{H}_l and \mathbf{G}_l (whose dimensions are $J_R \times M_S$ and $J_D \times M_R$, respectively) be the l th path channel matrix for the source-relay link and that for the relay-destination link, respectively. Therefore, $[\mathbf{H}_l]_{ij} = \alpha_{l,ij}$ and $[\mathbf{G}_l]_{ij} = \tilde{\alpha}_{l,ij}$ are the channel coefficients between the j th transmit antenna and the i th receive antenna for the first and second hops, respectively. These coefficients are assumed to remain constant during data transmission at both hops. This assumption is reasonable for slow-fading scenarios, e.g., UWB indoor communications [34] but not for fast-fading

TABLE I
EXAMPLES OF \mathbf{B} AND $\mathbf{V}_l(n)$ FOR RECEIVER-CSI-ASSISTED
RELAY SYSTEMS

M	N_b	\mathbf{B} of dimension $M \times N_b$	$\mathbf{V}_l(n)$ of dimension $N_b \times N_b$
2	2	$\begin{bmatrix} b_1 & -b_2 \\ b_2 & b_1 \end{bmatrix}$	$\begin{bmatrix} \alpha_{n1,l} & \alpha_{n2,l} \\ \alpha_{n2,l} & -\alpha_{n1,l} \end{bmatrix}$
3	4	$\begin{bmatrix} b_1 & -b_2 & -b_3 & -b_4 \\ b_2 & b_1 & b_4 & -b_3 \\ b_3 & -b_4 & b_1 & b_2 \end{bmatrix}$	$\begin{bmatrix} \alpha_{n1,l} & \alpha_{n2,l} & \alpha_{n3,l} & 0 \\ \alpha_{n2,l} & -\alpha_{n1,l} & 0 & \alpha_{n3,l} \\ \alpha_{n3,l} & 0 & -\alpha_{n1,l} & -\alpha_{n2,l} \\ 0 & -\alpha_{n3,l} & \alpha_{n2,l} & -\alpha_{n1,l} \end{bmatrix}$
4	4	$\begin{bmatrix} b_1 & -b_2 & -b_3 & -b_4 \\ b_2 & b_1 & b_4 & -b_3 \\ b_3 & -b_4 & b_1 & b_2 \\ b_4 & b_3 & -b_2 & b_1 \end{bmatrix}$	$\begin{bmatrix} \alpha_{n1,l} & \alpha_{n2,l} & \alpha_{n3,l} & \alpha_{n4,l} \\ \alpha_{n2,l} & -\alpha_{n1,l} & -\alpha_{n4,l} & \alpha_{n3,l} \\ \alpha_{n3,l} & \alpha_{n4,l} & -\alpha_{n1,l} & -\alpha_{n2,l} \\ \alpha_{n4,l} & -\alpha_{n3,l} & \alpha_{n2,l} & -\alpha_{n1,l} \end{bmatrix}$

scenarios. As mentioned in (1), we have $\alpha_{l,ij} = \sqrt{P}\varphi_{l,ij}$ and $\tilde{\alpha}_{l,ij} = \sqrt{\tilde{P}}\tilde{\varphi}_{l,ij}$. To make further analysis tractable, we assume that $\Omega_{l,ij} = \Omega_{l,i'j'}$ and $\tilde{\Omega}_{l,ij} = \tilde{\Omega}_{l,i'j'}$ for all l and $(i, j) \neq (i', j')$. For this reason and for notational simplicity, we omit the subscripts i and j of $\Omega_{l,ij}$, $\tilde{\Omega}_{l,ij}$ and the related variables in the rest of this paper. We ignore the direct link between the source and the destination due to the larger distance and additional path loss compared with the source-relay and relay-destination links.

III. RECEIVER-CSI-ASSISTED RELAY SYSTEMS

In these systems, the source has no CSI, but the relay and the destination have partial knowledge of the source-relay and relay-destination link channels, respectively, i.e., the relay knows the channel matrices $\{\mathbf{H}_l\}_{l=0}^{L-1}$ and the destination knows the channel matrices $\{\mathbf{G}_l\}_{l=0}^{L-1}$, where $L < L_t$. In the following, we describe decouple-and-forward (DCF) relaying⁴ and DF relaying schemes for such systems.

A. DCF Relaying

In this scheme, the source with multiple transmit antennas employs space-time block codes that are obtained from the real orthogonal design [36], as outlined in [37]. Let \mathbf{B} be the space-time block-coded data matrix whose dimension is $M \times N_c$, where N_c is the block length of the corresponding space-time block code. If binary data bits $\{b_k\}_{k=1}^{N_b}$ are transmitted with this matrix, then the code rate is N_b/N_c . In what follows, we concentrate on the space-time block-coded data matrices with the full code rate, i.e., $N_c = N_b$. Such matrices for two, three, and four transmit antennas are shown in Table I. Let us define $\mathbf{w}(t, i) = [w(t - N_b(i-1)T_f) \ w(t - N_b(i-1)T_f - T_f) \ \cdots \ w(t - N_b(i-1)T_f - (N_b-1)T_f)]^\dagger$, where T_f is the pulse repetition period and i will be stated in (5). To preclude intersymbol interference (ISI), we choose T_f

⁴Although a similar DCF relaying scheme was presented in [35], it is designed for dual-hop narrowband transmissions. In addition, it should be pointed out that, in the single-input-single-output (SISO) case, i.e., the source, relay, and destination have only one antenna, the DCF relaying scheme in this paper can be viewed as the AF relaying scheme for the receiver-CSI-assisted relay systems.

such that $T_f \geq L_t T_w$. In the first hop, the transmitted signal vector at the source can be modeled as

$$\mathbf{x}_S(t) = \sqrt{\frac{E_{f,S}}{M_S}} \sum_{i=1}^{N_f} \mathbf{B}_S \mathbf{w}(t, i) \quad (5)$$

where \mathbf{B}_S is the $M_S \times N_b$ space-time block-coded data matrix, N_f is the number of transmitted pulses that represent one data bit, i is the index of such pulses, $E_{f,S} = E_{b,S}/N_f$ is the energy of the transmitted pulse, and $E_{b,S}$ is the bit energy.

At each receive antenna of the relay, a Rake receiver with L fingers, whose correlators use the pulse $w(t)$ as a template, is employed [38]. Corresponding to the l th finger, the correlator outputs for all the receive antennas and received data bits at the relay can be expressed in a matrix form as

$$\mathbf{Y}_{R,l}(i) = \sqrt{\frac{E_{f,S}}{M_S}} \mathbf{H}_l \mathbf{B}_S + \mathbf{N}_{R,l}(i) \quad (6)$$

$$l = 0, \dots, L-1, \quad i = 1, \dots, N_f$$

where $\mathbf{N}_{R,l}(i)$ is the $J_R \times N_b$ matrix of the additive white Gaussian noise (AWGN) with zero mean and double-sided PSD $N_0/2$. To decouple the received signal matrix $\mathbf{Y}_{R,l}(i)$, we define the matrix $\mathbf{V}_{R,l}(n)$, which satisfies

$$[\mathbf{H}_l]_n \mathbf{B}_S = \mathbf{b}^\dagger \mathbf{V}_{R,l}(n) \quad (7)$$

where $\mathbf{b} = [b_1 \ b_2 \ \cdots \ b_{N_b}]^\dagger$ is the vector of the transmitted bits and n denotes the index of receive antennas. Examples of $\mathbf{V}_{R,l}(n)$ are given in Table I. Because the relay was assumed to know the channel matrices $\{\mathbf{H}_l\}_{l=0}^{L-1}$, the matrices $\{\mathbf{V}_{R,l}(n)\}_{l=0}^{L-1}$ in (7) are known to the relay. Consequently, the decoupled data bits, which are denoted by $\mathbf{z}_R = [z_{R,1} \ z_{R,2} \ \cdots \ z_{R,N_b}]^\dagger$, can be obtained as

$$\mathbf{z}_R = \sum_{n=1}^{J_R} \sum_{i=1}^{N_f} \sum_{l=0}^{L-1} \mathbf{V}_{R,l}(n) [\mathbf{Y}_{R,l}(i)]_n^\dagger. \quad (8)$$

At the relay, the k th element of \mathbf{z}_R is normalized with respect to $E_{\mathbf{H}}[|z_{R,k}|^2] = N_f \mathcal{E}(E_{b,S} \mathcal{E}/M_S + N_0/2)$, where $\mathcal{E} = \sum_{l=0}^{L-1} \mathcal{E}_l$ and $\mathcal{E}_l = \|\mathbf{H}_l\|^2$. Then, all normalized elements, which are denoted by $\{\tilde{z}_{R,k}\}_{k=1}^{N_b}$, are encoded similar to the data bits $\{b_k\}_{k=1}^{N_b}$ at the source. Such normalization is used to ensure that the transmitted signal vector at the relay, as shown later in (9), has the same average power as the one at the source if $E_{f,R}$ in (9) is equal to $E_{f,S}$. Denote by $\tilde{\mathbf{Z}}_R$ the resulting space-time block-coded matrix whose dimension is $M_R \times N_b$. Based on this matrix, the transmitted signal vector at the relay in the second hop is represented by

$$\mathbf{x}_R(t) = \sqrt{\frac{E_{f,R}}{M_R}} \sum_{i=1}^{N_f} \tilde{\mathbf{Z}}_R \mathbf{w}(t - N_b N_f T_f, i) \quad (9)$$

where $E_{f,R} = E_{b,R}/N_f$ is the energy of the transmitted pulse and $E_{b,R}$ is the energy of $\tilde{z}_{R,k}$.

Likewise, a Rake receiver with L fingers is used at each receive antenna of the destination. For the l th finger, the $J_D \times N_b$

matrix of the correlator outputs can thus be written as

$$\mathbf{Y}_{D,l}(i) = \sqrt{\frac{E_{f,R}}{M_R}} \mathbf{G}_l \bar{\mathbf{Z}}_R + \mathbf{N}_{D,l}(i) \quad l = 0, \dots, L-1, \quad i = 1, \dots, N_f \quad (10)$$

where $\mathbf{N}_{D,l}(i)$ is the $J_D \times N_b$ matrix of the AWGN with the same statistical properties as the elements of $\mathbf{N}_{R,l}(i)$. Exploiting the partial knowledge of the CSI $\{\mathbf{G}_l\}_{l=0}^{L-1}$, the destination generates the matrices $\{\mathbf{V}_{D,l}(n)\}_{l=0}^{L-1}$, which satisfy (7) with $[\mathbf{H}_l]_n$ being replaced by $[\mathbf{G}_l]_n$, to decouple $\{\mathbf{Y}_{D,l}(i)\}_{l=0, i=1}^{L-1, N_f}$. Finally, the vector of the decision variables can be derived as follows:

$$\begin{aligned} \mathbf{z}_D &= \sum_{n=1}^{J_D} \sum_{i=1}^{N_f} \sum_{l=0}^{L-1} \mathbf{V}_{D,l}(n) [\mathbf{Y}_{D,l}(i)]_n^\dagger \\ &= [z_{D,1} \quad z_{D,2} \quad \dots \quad z_{D,N_b}]^\dagger. \end{aligned} \quad (11)$$

For analytical convenience, from now on, we assume equal power allocation between the source and the relay, i.e., $E_{b,S} = E_{b,R} = E_b/2$ where E_b represents the transmitted energy per bit for the whole relay system. Because $E_{f,S} = E_{f,R} = E_b/(2N_f)$, we use E_f to denote both $E_{f,S}$ and $E_{f,R}$ in the rest of this paper. After some straightforward calculations, the overall end-to-end signal-to-noise ratio (SNR) per bit, i.e., the SNR of $z_{D,k}$, is found to be

$$\begin{aligned} \gamma &= \frac{E_b^2 \mathcal{E} \mathcal{E}'}{M_R E_b N_0 \mathcal{E} + M_S E_b N_0 \mathcal{E}' + M_S M_R N_0^2} \\ &= \frac{A_1 \mathcal{E} \mathcal{E}'}{A_2 \mathcal{E} + A_3 \mathcal{E}' + A_4} \end{aligned} \quad (12)$$

where $\mathcal{E}' = \sum_{l=0}^{L-1} \mathcal{E}'_l$, $\mathcal{E}'_l = \|\mathbf{G}_l\|^2$, and $A_1 = E_b^2$, $A_2 = M_R E_b N_0$, $A_3 = M_S E_b N_0$, and $A_4 = M_S M_R N_0^2$ are introduced for convenience in the subsequent analysis. In Appendix A, the pdf's and cdf's of \mathcal{E} and \mathcal{E}' are provided, and it is shown that these functions can be found in closed form only for the *spatial uncorrelation case*. We focus on this case in the following discussion, whereas the more general case, i.e., the *spatial correlation case*, will be considered in Section V.

1) *Outage Probability*: One common measure of performance in fading channels is the outage probability, which is defined as

$$P_{\text{out}} = \Pr[\gamma \leq \gamma_{\text{th}}] \quad (13)$$

where γ_{th} is a prespecified SNR threshold. By inserting (12) into (13) and following the same analysis as in [39, Sec. III-A], we get

$$\begin{aligned} P_{\text{out}} &= \int_0^{\frac{A_3}{A_1} \gamma_{\text{th}}} f_{\mathcal{E}}(x) dx + \int_{\frac{A_3}{A_1} \gamma_{\text{th}}}^{\infty} F_{\mathcal{E}'} \left(\frac{\gamma_{\text{th}}(A_2 x + A_4)}{A_1 x - A_3 \gamma_{\text{th}}} \right) f_{\mathcal{E}}(x) dx \\ &= 1 - 2 \sum_{l=0}^{L-1} \sum_{k=1}^{\mu} \Delta \sum_{l'=0}^{L-1} \sum_{k'=1}^{\tilde{\mu}} \Delta' \frac{(\mathcal{C}_1 \gamma_{\text{th}} / \check{\gamma})^k}{(k-1)!} \end{aligned}$$

$$\begin{aligned} &\times \exp\left(-\frac{\gamma_{\text{th}}}{\check{\gamma}} (\mathcal{C}_1 + \mathcal{C}_2)\right) \sqrt{\frac{\mathcal{C}_2}{\mathcal{C}_1} \left(1 + \frac{1}{\gamma_{\text{th}}}\right)} \\ &\times \sum_{j_1=0}^{k'-1} \frac{(\mathcal{C}_2 \gamma_{\text{th}} / \check{\gamma})^{j_1}}{j_1!} \sum_{j_2=0}^{j_1} \binom{j_1}{j_2} \left[\frac{\mathcal{C}_1}{\mathcal{C}_2} \left(1 + \frac{1}{\gamma_{\text{th}}}\right) \right]^{\frac{j_2}{2}} \\ &\times \sum_{j_3=0}^{k-1} \binom{k-1}{j_3} \left[\frac{\mathcal{C}_2}{\mathcal{C}_1} \left(1 + \frac{1}{\gamma_{\text{th}}}\right) \right]^{\frac{j_3}{2}} \\ &\times \mathcal{K}_{j_3-j_2+1} \left(\frac{2}{\check{\gamma}} \sqrt{\mathcal{C}_1 \mathcal{C}_2 \gamma_{\text{th}} (1 + \gamma_{\text{th}})} \right) \end{aligned} \quad (14)$$

where $\mathcal{C}_1 = M_S / \Phi_l$, $\mathcal{C}_2 = M_R / \check{\Phi}_{l'}$, $\check{\gamma} = E_b / N_0$ is the transmitted SNR per bit, and μ , $\tilde{\mu}$, Φ_l , and $\check{\Phi}_{l'}$ are defined in Appendix A. The term Δ is the abbreviation for $\Delta(l, k, \mu, \{\Phi_q\}_{q=0}^{L-1})$ given in (51), and the term Δ' stands for $\Delta(l', k', \tilde{\mu}, \{\check{\Phi}_{q'}\}_{q'=0}^{L-1})$.

To get an insight into the effect of some parameters (e.g., the number of antennas) on the system performance based on (14), we consider the following special case.

For $M_S = J_R = M_R = 1$, $L = 1$, $m = \tilde{m} = 1$, and $\Phi_0 = \check{\Phi}_0$, (14) reduces to

$$\begin{aligned} P_{\text{out}} &= 1 - \frac{2\mathcal{C}_1 \gamma_{\text{th}}}{\check{\gamma}} \sqrt{1 + \frac{1}{\gamma_{\text{th}}}} \exp\left(-\frac{2\mathcal{C}_1 \gamma_{\text{th}}}{\check{\gamma}}\right) \sum_{j_1=0}^{\tilde{\mu}-1} \frac{(\mathcal{C}_1 \gamma_{\text{th}} / \check{\gamma})^{j_1}}{j_1!} \\ &\times \sum_{j_2=0}^{j_1} \binom{j_1}{j_2} \left(1 + \frac{1}{\gamma_{\text{th}}}\right)^{\frac{j_2}{2}} \mathcal{K}_{j_2-1} \left(\frac{2\mathcal{C}_1}{\check{\gamma}} \sqrt{\gamma_{\text{th}} (1 + \gamma_{\text{th}})} \right). \end{aligned} \quad (15)$$

Note that $\tilde{\mu} = M_R J_D \tilde{m}$. It is obvious in (15) that increasing the number of receive antennas at the destination (J_D) increases $\tilde{\mu}$ and the summation, thereby decreasing the outage probability.

In more general cases, the benefit of multiple-antenna deployment will be demonstrated by numerical examples in Section V.

2) *AOF*: We use the AOF to quantify the severity of fading at the output of the DCF relay system. This measure is given by [28, eq. (2.5)]

$$\text{AOF} = \frac{\mathbb{E}[\gamma^2]}{(\mathbb{E}[\gamma])^2} - 1 \quad (16)$$

where

$$\mathbb{E}[\gamma^n] = \int_0^{\infty} x^n f_{\gamma}(x) dx \quad (17)$$

is the n th-order moment of γ . To calculate the AOF, we first need to find the pdf $f_{\gamma}(x)$. This pdf is given in (57) in Appendix B. To the best of the authors' knowledge, however, the closed-form solution to (17) is not available. One option is to develop a tight approximation of (17). In the following discussion, we assume that the transmitted SNR per bit $\check{\gamma}$ is large enough such that $((\mathcal{E}/M_S) + (\mathcal{E}'/M_R))\check{\gamma} \gg 1$. Under this assumption, the end-to-end SNR per bit can be approximated as

$$\gamma \approx \frac{A_1 \mathcal{E} \mathcal{E}'}{A_2 \mathcal{E} + A_3 \mathcal{E}'} \triangleq \gamma_{\text{ap}}. \quad (18)$$

Following the same procedure as in Section III-A1, the cdf

$F_{\gamma_{\text{ap}}}(x) = \Pr[\gamma_{\text{ap}} \leq x]U(x)$ is obtained as

$$\begin{aligned}
F_{\gamma_{\text{ap}}}(x) &= \left[1 - 2 \sum_{l=0}^{L-1} \sum_{k=1}^{\mu} \Delta \sum_{l'=0}^{L-1} \sum_{k'=1}^{\bar{\mu}} \Delta' \sqrt{\frac{\mathcal{C}_2}{\mathcal{C}_1}} \frac{(\mathcal{C}_1 x / \check{\gamma})^k}{(k-1)!} \right. \\
&\quad \times \exp\left(-\frac{x}{\check{\gamma}}(\mathcal{C}_1 + \mathcal{C}_2)\right) \sum_{j_1=0}^{k'-1} \frac{(\mathcal{C}_2 x / \check{\gamma})^{j_1}}{j_1!} \\
&\quad \times \sum_{j_2=0}^{j_1} \binom{j_1}{j_2} \left(\frac{\mathcal{C}_1}{\mathcal{C}_2}\right)^{\frac{j_2}{2}} \sum_{j_3=0}^{k-1} \binom{k-1}{j_3} \left(\frac{\mathcal{C}_2}{\mathcal{C}_1}\right)^{\frac{j_3}{2}} \\
&\quad \left. \times \mathcal{K}_{j_3-j_2+1} \left(\frac{2x}{\check{\gamma}} \sqrt{\mathcal{C}_1 \mathcal{C}_2}\right) \right] U(x). \quad (19)
\end{aligned}$$

Based on (19), we can obtain

$$\begin{aligned}
f_{\gamma_{\text{ap}}}(x) &= 2 \sum_{l=0}^{L-1} \sum_{k=1}^{\mu} \Delta \sum_{l'=0}^{L-1} \sum_{k'=1}^{\bar{\mu}} \Delta' \sqrt{\frac{\mathcal{C}_2}{\mathcal{C}_1}} \frac{(\mathcal{C}_1 x / \check{\gamma})^k}{(k-1)!} \\
&\quad \times \exp\left(-\frac{x}{\check{\gamma}}(\mathcal{C}_1 + \mathcal{C}_2)\right) \sum_{j_1=0}^{k'-1} \frac{(\mathcal{C}_2 x / \check{\gamma})^{j_1}}{j_1!} \\
&\quad \times \sum_{j_2=0}^{j_1} \binom{j_1}{j_2} \left(\frac{\mathcal{C}_1}{\mathcal{C}_2}\right)^{\frac{j_2}{2}} \sum_{j_3=0}^{k-1} \binom{k-1}{j_3} \left(\frac{\mathcal{C}_2}{\mathcal{C}_1}\right)^{\frac{j_3}{2}} \\
&\quad \times \left\{ \left(\frac{\mathcal{C}_1 + \mathcal{C}_2}{\check{\gamma}} - \frac{j_1 + k}{x}\right) \mathcal{K}_{j_3-j_2+1} \left(\frac{2x}{\check{\gamma}} \sqrt{\mathcal{C}_1 \mathcal{C}_2}\right) \right. \\
&\quad \left. + \frac{\sqrt{\mathcal{C}_1 \mathcal{C}_2}}{\check{\gamma}} \left[\mathcal{K}_{j_3-j_2} \left(\frac{2x}{\check{\gamma}} \sqrt{\mathcal{C}_1 \mathcal{C}_2}\right) \right. \right. \\
&\quad \left. \left. + \mathcal{K}_{j_3-j_2+2} \left(\frac{2x}{\check{\gamma}} \sqrt{\mathcal{C}_1 \mathcal{C}_2}\right) \right] \right\} U(x). \quad (20)
\end{aligned}$$

With the aid of [27, eq. (6.621.3)], the high-SNR approximation of the n th-order moment of γ can be derived as in (21), shown at the bottom of the page. Here, $c_1 = j_1 + k$, and $c_2 = j_3 - j_2 + 1$. Using (16) and (21), the approximate AOF is obtained. In

Section V, we will see that this AOF closely matches the AOF that is evaluated from $f_{\gamma}(x)$ through simulations.

3) *BER*: Another important performance measure that characterizes the end-to-end link quality is the *average BER*. It is given by [28, eq. (5.1)]

$$P_e = \int_0^{\infty} Q(\sqrt{x}) f_{\gamma}(x) dx. \quad (22)$$

Similar to the AOF, there is no closed-form solution to (22) with $f_{\gamma}(x)$ of (57). By using the aforementioned high-SNR assumption, however, the BER can approximately be evaluated as follows:

$$\begin{aligned}
P_e &\approx \int_0^{\infty} Q(\sqrt{x}) f_{\gamma_{\text{ap}}}(x) dx = \Pr[\sqrt{\gamma_{\text{ap}}} < \mathcal{Y}] \\
&= \int_0^{\infty} F_{\gamma_{\text{ap}}}(y^2) f_{\mathcal{Y}}(y) dy \\
&= \frac{1}{2} - \sqrt{\check{\gamma}} \sum_{l=0}^{L-1} \sum_{k=1}^{\mu} \Delta \sum_{l'=0}^{L-1} \sum_{k'=1}^{\bar{\mu}} \Delta' \frac{\mathcal{C}_1^k}{(k-1)!} \\
&\quad \times \sum_{j_1=0}^{k'-1} \frac{\mathcal{C}_2^{j_1}}{j_1!} \sum_{j_2=0}^{j_1} \binom{j_1}{j_2} \sum_{j_3=0}^{k-1} \binom{k-1}{j_3} \\
&\quad \times \frac{2^{c_1+3c_2} \mathcal{C}_2^{c_2} \Gamma(c_1 + c_2 + 1/2) \Gamma(c_1 - c_2 + 1/2)}{\Gamma(c_1 + 1) (\check{\gamma} + 2(\sqrt{\mathcal{C}_1} + \sqrt{\mathcal{C}_2})^2)^{c_1+c_2+1/2}} \\
&\quad \times {}_2F_1\left(c_1 + c_2 + \frac{1}{2}, c_2 + \frac{1}{2}; c_1 + 1; \right. \\
&\quad \left. \frac{\check{\gamma} + 2(\sqrt{\mathcal{C}_1} - \sqrt{\mathcal{C}_2})^2}{\check{\gamma} + 2(\sqrt{\mathcal{C}_1} + \sqrt{\mathcal{C}_2})^2}\right) \quad (23)
\end{aligned}$$

where the first equality is obtained by letting \mathcal{Y} be a standard normal random variable and using [28, eq. (4.1)], and the last equality is obtained by using [27, eq. (6.621.3)].

$$\begin{aligned}
\mathbb{E}[\gamma^n] &\approx \int_0^{\infty} x^n f_{\gamma_{\text{ap}}}(x) dx \\
&= 2\sqrt{\pi} \check{\gamma}^n \sum_{l=0}^{L-1} \sum_{k=1}^{\mu} \Delta \sum_{l'=0}^{L-1} \sum_{k'=1}^{\bar{\mu}} \Delta' \frac{\mathcal{C}_1^k}{(k-1)!} \sum_{j_1=0}^{k'-1} \frac{\mathcal{C}_2^{j_1}}{j_1!} \sum_{j_2=0}^{j_1} \binom{j_1}{j_2} \sum_{j_3=0}^{k-1} \binom{k-1}{j_3} \frac{\Gamma(c_1 + c_2 + n) \Gamma(c_1 - c_2 + n) 2^{2c_2} \mathcal{C}_2^{c_2}}{\Gamma(c_1 + n + 3/2) (\sqrt{\mathcal{C}_1} + \sqrt{\mathcal{C}_2})^{2(c_1+c_2+n)}} \\
&\quad \times \left\{ \frac{((c_1 + n)^2 - c_2^2) (\mathcal{C}_1 + \mathcal{C}_2)}{(\sqrt{\mathcal{C}_1} + \sqrt{\mathcal{C}_2})^2} {}_2F_1\left(c_1 + c_2 + n + 1, c_2 + \frac{1}{2}; c_1 + n + \frac{3}{2}; \left(\frac{\sqrt{\mathcal{C}_1} - \sqrt{\mathcal{C}_2}}{\sqrt{\mathcal{C}_1} + \sqrt{\mathcal{C}_2}}\right)^2\right) \right. \\
&\quad \left. + \frac{1}{4} (c_1 - c_2 + n)(c_1 - c_2 + n + 1) {}_2F_1\left(c_1 + c_2 + n, c_2 - \frac{1}{2}; c_1 + n + \frac{3}{2}; \left(\frac{\sqrt{\mathcal{C}_1} - \sqrt{\mathcal{C}_2}}{\sqrt{\mathcal{C}_1} + \sqrt{\mathcal{C}_2}}\right)^2\right) \right. \\
&\quad \left. + \frac{4(c_1 + c_2 + n)(c_1 + c_2 + n + 1) \mathcal{C}_1 \mathcal{C}_2}{(\sqrt{\mathcal{C}_1} + \sqrt{\mathcal{C}_2})^4} {}_2F_1\left(c_1 + c_2 + n + 2, c_2 + \frac{3}{2}; c_1 + n + \frac{3}{2}; \left(\frac{\sqrt{\mathcal{C}_1} - \sqrt{\mathcal{C}_2}}{\sqrt{\mathcal{C}_1} + \sqrt{\mathcal{C}_2}}\right)^2\right) \right. \\
&\quad \left. - (j_1 + k)(c_1 + n + 1/2) {}_2F_1\left(c_1 + c_2 + n, c_2 + \frac{1}{2}; c_1 + n + \frac{1}{2}; \left(\frac{\sqrt{\mathcal{C}_1} - \sqrt{\mathcal{C}_2}}{\sqrt{\mathcal{C}_1} + \sqrt{\mathcal{C}_2}}\right)^2\right) \right\} \quad (21)
\end{aligned}$$

B. DF Relaying

In the DF relaying scheme, the transmitted and received signals for the first hop are the same as in (5) and (6), respectively. Such received signals are decoupled and combined to produce the decoupled data bits as described in (8). Subsequently, the relay makes hard decisions on the decoupled bits and encodes them in a similar manner as the source encodes the data bits. This yields the matrix $\hat{\mathbf{B}}_R$ of dimension $M_R \times N_b$. As will be shown in Section V, such a hard decision leads to better performance (at the cost of higher complexity) than the DCF relaying scheme. In the second hop, the transmitted signals at the relay and the received signals at the destination can be represented, respectively, as in (9) and (10), with $\bar{\mathbf{Z}}_R$ being replaced by $\hat{\mathbf{B}}_R$. Last, the decision variables can be obtained as in (11). It is straightforward to show that the received SNRs per bit for the first and second hops, respectively, are

$$\gamma_1 = \frac{\mathcal{E}\check{\gamma}}{M_S} \quad (24a)$$

$$\gamma_2 = \frac{\mathcal{E}'\check{\gamma}}{M_R}. \quad (24b)$$

1) *Outage Probability*: An outage occurs if either the source–relay or relay–destination link is in outage. Therefore, we have

$$\begin{aligned} P_{\text{out}} &= \Pr[\min(\gamma_1, \gamma_2) \leq \gamma_{\text{th}}] \\ &= 1 - \Pr[\gamma_1 > \gamma_{\text{th}}] \Pr[\gamma_2 > \gamma_{\text{th}}] \\ &= 1 - \left[1 - F_{\mathcal{E}}\left(\frac{M_S}{\check{\gamma}}\gamma_{\text{th}}\right) \right] \left[1 - F_{\mathcal{E}'}\left(\frac{M_R}{\check{\gamma}}\gamma_{\text{th}}\right) \right] \\ &= 1 - \left[\sum_{l=0}^{L-1} \sum_{k=1}^{\mu} \Delta \frac{\Gamma(k, \mathcal{C}_1 \gamma_{\text{th}} / \check{\gamma})}{(k-1)!} \right] \\ &\quad \times \left[\sum_{l'=0}^{L-1} \sum_{k'=1}^{\bar{\mu}} \Delta' \frac{\Gamma(k', \mathcal{C}_2 \gamma_{\text{th}} / \check{\gamma})}{(k'-1)!} \right]. \end{aligned} \quad (25)$$

2) *AOF*: The AOF for the DF relaying scheme can be defined as

$$\text{AOF} = \frac{\mathbb{E}[\gamma_{\text{eq}}^2]}{(\mathbb{E}[\gamma_{\text{eq}}])^2} - 1 \quad (26)$$

where

$$\mathbb{E}[\gamma_{\text{eq}}^n] = \int_0^{\infty} x^n f_{\gamma_{\text{eq}}}(x) dx \quad (27)$$

is the n th-order moment of

$$\gamma_{\text{eq}} = [Q^{-1}(P_e(\gamma_1, \gamma_2))]^2 \quad (28)$$

which represents the *equivalent* end-to-end SNR of the source–relay and relay–destination links [40, eq. (6)]. $P_e(\gamma_1, \gamma_2) = P_{e1}(\gamma_1) + P_{e2}(\gamma_2) - 2P_{e1}(\gamma_1)P_{e2}(\gamma_2)$ is the *conditional* BER for this scheme [40, eq. (5)], and $P_{e1}(\gamma_1) = Q(\sqrt{\gamma_1})$ and $P_{e2}(\gamma_2) = Q(\sqrt{\gamma_2})$ are the conditional BERs of both links. However, because it is difficult to find an exact expression

of the pdf of γ_{eq} in (28), we approximate γ_{eq} , as given in [40, eq. (7)], by

$$\gamma_{\text{eq}} \simeq \min(\gamma_1, \gamma_2) \triangleq \gamma_{\min}. \quad (29)$$

Taking the derivative of (25) with respect to γ_{th} , we obtain the pdf for γ_{\min} as

$$\begin{aligned} f_{\gamma_{\min}}(x) &= \sum_{l=0}^{L-1} \sum_{k=1}^{\mu} \frac{\Delta}{(k-1)!} \sum_{l'=0}^{L-1} \sum_{k'=1}^{\bar{\mu}} \frac{\Delta'}{(k'-1)!} \\ &\quad \times \left[\left(\frac{\mathcal{C}_1}{\check{\gamma}} \right)^k x^{k-1} \exp\left(-\frac{\mathcal{C}_1 x}{\check{\gamma}}\right) \Gamma\left(k', \frac{\mathcal{C}_2 x}{\check{\gamma}}\right) \right. \\ &\quad \left. + \left(\frac{\mathcal{C}_2}{\check{\gamma}} \right)^{k'} x^{k'-1} \exp\left(-\frac{\mathcal{C}_2 x}{\check{\gamma}}\right) \Gamma\left(k, \frac{\mathcal{C}_1 x}{\check{\gamma}}\right) \right] U(x). \end{aligned} \quad (30)$$

From (27) and (29), it follows that the n th-order moment of γ_{eq} can be approximated as

$$\begin{aligned} \mathbb{E}[\gamma_{\text{eq}}^n] &\simeq \int_0^{\infty} x^n f_{\gamma_{\min}}(x) dx = \sum_{l=0}^{L-1} \sum_{k=1}^{\mu} \Delta \sum_{l'=0}^{L-1} \sum_{k'=1}^{\bar{\mu}} \Delta' \\ &\quad \times \frac{(\check{\gamma}/(\mathcal{C}_1 + \mathcal{C}_2))^n \Gamma(n+k+k')}{(k-1)!(k'-1)!(\mathcal{C}_2/\mathcal{C}_1 + 1)^k (\mathcal{C}_1/\mathcal{C}_2 + 1)^{k'}} \\ &\quad \times \left[\frac{1}{(n+k)} {}_2F_1\left(1, n+k+k'; n+k+1; \frac{\mathcal{C}_1}{\mathcal{C}_1 + \mathcal{C}_2}\right) \right. \\ &\quad \left. + \frac{1}{(n+k')} {}_2F_1\left(1, n+k+k'; n+k'+1; \frac{\mathcal{C}_2}{\mathcal{C}_1 + \mathcal{C}_2}\right) \right] \end{aligned} \quad (31)$$

where we have used [27, eq. (6.455.1)] for the equality. Using (26) and (31), the approximate AOF is obtained. In Section V, the numerical results will demonstrate that this AOF matches well with the AOF obtained from (26) through simulations.

3) *BER*: The average BER for this relaying scheme is given by [11, eq. (17)]

$$P_e = P_{e1} + P_{e2} - 2P_{e1}P_{e2} \quad (32)$$

where P_{e1} and P_{e2} are the average BERs of the source–relay and relay–destination links, respectively. According to (24) and (48), the pdf of γ_1 is given by $f_{\gamma_1}(x) = (M_S/\check{\gamma}) f_{\mathcal{E}}((M_S/\check{\gamma})x) = (M_S/\check{\gamma}) \sum_{l=0}^{L-1} \sum_{k=1}^{\mu} \Delta f_{\mathcal{E}_l}((M_S/\check{\gamma})x; k, \Phi_l)$. Hence, we can derive P_{e1} as follows:

$$\begin{aligned} P_{e1} &= \int_0^{\infty} Q(\sqrt{x}) f_{\gamma_1}(x) dx = \frac{1}{2\sqrt{\pi}} \sum_{l=0}^{L-1} \sum_{k=1}^{\mu} \Delta \frac{(\mathcal{C}_1/\check{\gamma})^k}{(k-1)!} \\ &\quad \times \int_0^{\infty} x^{k-1} \Gamma\left(\frac{1}{2}, \frac{x}{2}\right) \exp\left(-\frac{\mathcal{C}_1 x}{\check{\gamma}}\right) dx \\ &= \frac{1}{2} \sqrt{\frac{\check{\gamma}}{\pi}} \sum_{l=0}^{L-1} \sum_{k=1}^{\mu} \Delta \frac{\Gamma(k+1/2)}{k! \sqrt{\check{\gamma}} + 2\mathcal{C}_1} \left(\frac{2}{\check{\gamma}/\mathcal{C}_1 + 2} \right)^k \\ &\quad \times {}_2F_1\left(1, k + \frac{1}{2}; k+1; \frac{2}{\check{\gamma}/\mathcal{C}_1 + 2}\right) \end{aligned} \quad (33)$$

where we have used the fact that $Q(x) = \text{erfc}(x/\sqrt{2})/2$ and [27, eq. (8.359.3)] to obtain the second equality, and we have used [27, eq. (6.455.1)] for the last equality. Similarly, the pdf of γ_2 is given by $f_{\gamma_2}(x) = (M_R/\tilde{\gamma}) \sum_{l'=0}^{L-1} \sum_{k'=1}^{\tilde{\mu}} \Delta' f_{\mathcal{E}'_l}((M_R/\tilde{\gamma})x; k', \tilde{\Phi}_{l'})$, and we get

$$P_{e2} = \frac{1}{2} \sqrt{\frac{\tilde{\gamma}}{\pi}} \sum_{l'=0}^{L-1} \sum_{k'=1}^{\tilde{\mu}} \Delta' \frac{\Gamma(k'+1/2)}{k'! \sqrt{\tilde{\gamma} + 2\mathcal{C}_2}} \left(\frac{2}{\tilde{\gamma}/\mathcal{C}_2 + 2} \right)^{k'} \times {}_2F_1 \left(1, k' + \frac{1}{2}; k' + 1; \frac{2}{\tilde{\gamma}/\mathcal{C}_2 + 2} \right). \quad (34)$$

IV. TRANSMITTER-CSI-ASSISTED RELAY SYSTEMS

In contrast to the receiver-CSI-assisted relay systems, the source and relay in these systems have partial knowledge of the source-relay and relay-destination link channels, respectively, i.e., the source knows the channel matrices $\{\mathbf{H}_l\}_{l=0}^{L-1}$ and the relay knows the channel matrices $\{\mathbf{G}_l\}_{l=0}^{L-1}$. In the following, we focus on two kinds of relaying schemes: 1) AF relaying and 2) detect-and-forward (DTF) relaying.

A. AF Relaying

In this relaying scheme, the pre-Rake technique [41], [42] is used. In the first hop, the transmitted signal vector at the source can be modeled as

$$\mathbf{x}_S(t) = \sqrt{\frac{E_f}{\mathcal{E}}} \sum_{i=1}^{N_f} \sum_{l=0}^{L-1} \mathbf{H}_{L-1-l}^\dagger \mathbf{1}_{J_R} \mathbf{b}^\dagger \mathbf{w}(t, i, l) \quad (35)$$

where $\mathbf{w}(t, i, l) = [w(t - N_b(i-1)T_f - lT_w) \quad w(t - N_b(i-1)T_f - T_f - lT_w) \quad \dots \quad w(t - N_b(i-1)T_f - (N_b-1)T_f - lT_w)]^\dagger$. It can easily be shown that the total transmitted energy per bit from the source is the same as in the aforementioned relaying schemes. Note from (35) that all the antennas at the source transmit the same data bits b_k ($k = 1, 2, \dots, N_b$) at the same time. Furthermore, the source convolves the data bits with the time-reversed version of the partial CIRs for the first-hop links. This procedure results in a strong peak of the total received signal at each receive antenna of the relay,⁵ and then, only a matched filter [matched to the UWB pulse $w(t)$] is needed to receive this path [42]. To gain a better understanding, let us first consider the received signals at the relay, after passing through the matched filter and sampling, in a matrix form as

$$\mathbf{Y}_{R,l}(i) = \sqrt{\frac{E_f}{\mathcal{E}}} \mathbf{H}_l * \mathbf{H}_{L-1-l}^\dagger \mathbf{1}_{J_R} \mathbf{b}^\dagger + \mathbf{N}_{R,l}(i) \quad l = 0, \dots, L-1, \quad i = 1, \dots, N_f. \quad (36)$$

One can show that all diagonal elements of $\mathbf{H}_l * \mathbf{H}_{L-1-l}^\dagger$ achieve their peaks at $l = L-1$. Therefore, to estimate $\{b_k\}_{k=1}^{N_b}$, the relay only needs

$$\mathbf{Y}_{R,L-1}(i) = \sqrt{\frac{E_f}{\mathcal{E}}} \sum_{k=0}^{L-1} \mathbf{H}_k \mathbf{H}_k^\dagger \mathbf{1}_{J_R} \mathbf{b}^\dagger + \mathbf{N}_{R,L-1}(i) \quad i = 1, \dots, N_f. \quad (37)$$

⁵This holds because we assume the same tap length for all the CIRs.

The estimate of the data bit vector \mathbf{b} at the relay is given by

$$\mathbf{z}_R = \sum_{n=1}^{J_R} \sum_{i=1}^{N_f} [\mathbf{Y}_{R,L-1}(i)]_n^\dagger. \quad (38)$$

Subsequently, all the elements of \mathbf{z}_R are normalized with respect to $E_{\mathbf{H}}[|z_{R,k}|^2] = N_f [E_b(\mathcal{E} + \mathcal{I})^2/\mathcal{E} + (J_R N_0/2)]$, where $\mathcal{I} = \sum_{l=0}^{L-1} \sum_{n=1}^{J_R} \sum_{n'=1}^{M_S} \sum_{j=1, j \neq n}^{J_R} [\mathbf{H}_l]_{jn'} [\mathbf{H}_l]_{nn'}$, yielding $\{\bar{z}_{R,k}\}_{k=1}^{N_b}$.

In the second hop, the transmitted signal vector at the relay can be expressed as

$$\mathbf{x}_R(t) = \sqrt{\frac{E_f}{\mathcal{E}'}} \sum_{i=1}^{N_f} \sum_{l=0}^{L-1} \mathbf{G}_{L-1-l}^\dagger \mathbf{1}_{J_D} \bar{\mathbf{z}}_R^\dagger \mathbf{w}(t - N_b N_f T_f, i, l) \quad (39)$$

where $\bar{\mathbf{z}}_R = [\bar{z}_{R,1} \quad \bar{z}_{R,2} \quad \dots \quad \bar{z}_{R,N_b}]^\dagger$. Similar to (37), after receiving the signals and passing them through the matched filter, the destination requires only the following sampled outputs:

$$\mathbf{Y}_{D,L-1}(i) = \sqrt{\frac{E_f}{\mathcal{E}'}} \sum_{k=0}^{L-1} \mathbf{G}_k \mathbf{G}_k^\dagger \mathbf{1}_{J_D} \bar{\mathbf{z}}_R^\dagger + \mathbf{N}_{D,L-1}(i) \quad i = 1, \dots, N_f. \quad (40)$$

Accordingly, the destination can form the vector of the decision variables as

$$\mathbf{z}_D = \sum_{n=1}^{J_D} \sum_{i=1}^{N_f} [\mathbf{Y}_{D,L-1}(i)]_n^\dagger. \quad (41)$$

After some calculations, the overall end-to-end SNR per bit is found as

$$\gamma = \frac{[E_b(\mathcal{E} + \mathcal{I})(\mathcal{E}' + \mathcal{I}')]^2}{J_D E_b N_0 \mathcal{E}' (\mathcal{E} + \mathcal{I})^2 + J_R E_b N_0 \mathcal{E} (\mathcal{E}' + \mathcal{I}')^2 + J_R J_D \mathcal{E} \mathcal{E}' N_0^2} \quad (42)$$

where $\mathcal{I}' = \sum_{l=0}^{L-1} \sum_{n=1}^{J_D} \sum_{n'=1}^{M_R} \sum_{j=1, j \neq n}^{J_D} [\mathbf{G}_l]_{jn'} [\mathbf{G}_l]_{nn'}$. Note that \mathcal{I} (and/or \mathcal{I}') vanishes for $J_R = 1$ (and/or $J_D = 1$).

1) *Outage Probability*: Similar to the analysis in Section III-A1, we need the cdf's of \mathcal{I} and \mathcal{I}' to derive the outage probability that corresponds to γ in (42). Unfortunately, it is difficult, if not impossible, to find those cdf's. The outage probability is therefore determined based on (13) through simulations, except for the case where $J_R = J_D = 1$. In this case, (42) reduces to (12), with M_S and M_R being replaced by J_R and J_D , respectively. Hence, the outage probability can be expressed as in (14), with \mathcal{C}_1 and \mathcal{C}_2 being replaced by $\mathcal{C}_3 = J_R/\Phi_l$ and $\mathcal{C}_4 = J_D/\tilde{\Phi}_{l'}$, respectively.

2) *AOF*: In the case of $J_R = J_D = 1$, we use the high-SNR approximation in Section III-A2 for γ in (42). Consequently, (42) reduces to (18), with A_2 and A_3 being replaced by $A_5 = J_D E_b N_0$ and $A_6 = J_R E_b N_0$, respectively. Following the same procedure as in (21), the approximation of the n th-order moment of γ in this case is obtained as the second line of (21), with \mathcal{C}_1 and \mathcal{C}_2 being replaced by \mathcal{C}_3 and \mathcal{C}_4 , respectively. In other cases, the n th-order moment is computed through simulations. Finally, the corresponding AOF is calculated according to (16).

3) *BER*: Likewise, the average BER is calculated through simulations, except for the case where $J_R = J_D = 1$. In this case, the approximate average BER under the high-SNR assumption can be obtained as in (23), with C_1 and C_2 being replaced by C_3 and C_4 , respectively.

B. DTF Relaying

In the DTF relaying scheme, the transmitted and received signals for the first hop are the same as in (35) and (37), respectively. The relay performs the data detection by producing the estimates of the transmitted bits as in (38) and making hard decisions on them. The vector of the detected bits is given by $\hat{\mathbf{b}}_R = \text{sign}(\mathbf{z}_R)$. Those hard decisions result in superior performance compared with the AF relaying scheme, as will be shown in the following section. In the second hop, the transmitted signals at the relay and the received signals at the destination can be expressed, respectively, as in (39) and (40), with $\bar{\mathbf{z}}_R$ being replaced by $\hat{\mathbf{b}}_R$. Finally, the decision variables can be obtained as in (41). It is straightforward to show that the received SNRs per bit for the first and second hops, respectively, are

$$\gamma_1 = \frac{(\mathcal{E} + \mathcal{I})\check{\gamma}}{J_R} \quad (43a)$$

$$\gamma_2 = \frac{(\mathcal{E}' + \mathcal{I}')\check{\gamma}}{J_D}. \quad (43b)$$

1) *Outage Probability*: Comparing (43) with (24), we observe that they are of similar form. Hence, we can follow the approach that was taken to derive the outage probability for the DF relaying scheme. In the case of $J_R = J_D = 1$, we obtain the outage probability as in (25), with C_1 and C_2 being replaced by C_3 and C_4 , respectively. In other cases, the outage probability is obtained through simulations.

2) *AOF*: Due to the aforementioned similarity, we follow the approach in Section III-B2 in deriving the AOF for this scheme. When $J_R = J_D = 1$, the AOF is approximately calculated using (26) and (31), with C_1 and C_2 being replaced by C_3 and C_4 , respectively. Otherwise, the AOF is obtained through simulations.

3) *BER*: We follow the approach in Section III-B3 in deriving the average BER for this scheme. When $J_R = J_D = 1$, the BER is obtained as in (32), where P_{e1} and P_{e2} are the same as in (33) and (34), with C_1 and C_2 being replaced by C_3 and C_4 , respectively. Otherwise, the BER is obtained through simulations.

V. NUMERICAL RESULTS AND DISCUSSION

In this section, numerical examples of the results that are derived in this paper are presented. The system setup is depicted in Fig. 1, where we assume that the source and the destination are separated by a distance of 8 m, and the relay is located halfway between them. The total multipath gains P and \tilde{P} are calculated according to the UWB path loss model described in [29, eq. (1)]. In generating the UWB energy-normalized channel coefficients $\{\varphi_l\}_{l=0}^{L-1}$ and $\{\tilde{\varphi}_l\}_{l=0}^{L-1}$, we assume that $L_t = 50$, $m = \tilde{m} = 2$, $\Omega_0 = \tilde{\Omega}_0 = 0.054$, and $\varpi = \tilde{\varpi} = 0.95$ [25]. For illustration purposes, we only consider the cases where $M_S, J_R, M_R,$ and $J_D \leq 2$, except in Section V-D.

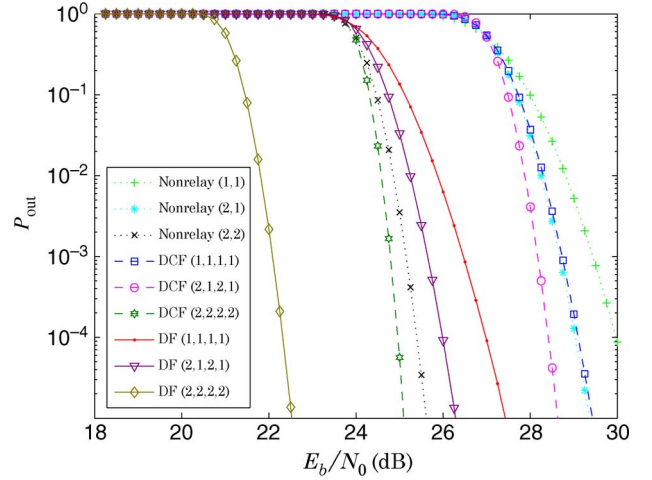


Fig. 2. Outage probabilities of the receiver-CSI-assisted nonrelay and relay systems, all with $L = 20$.

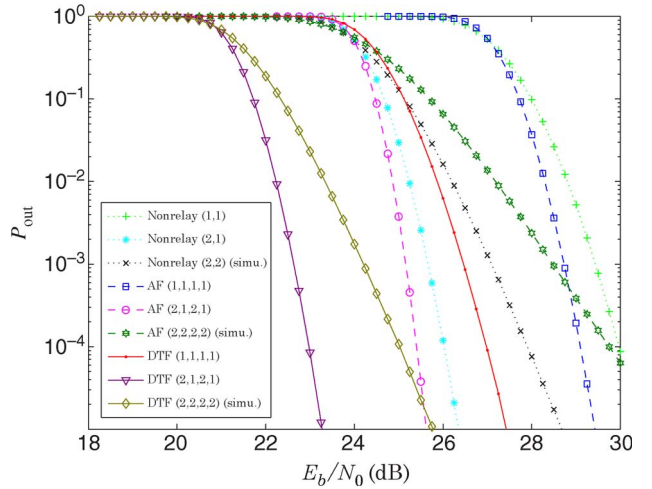


Fig. 3. Outage probabilities of the transmitter-CSI-assisted nonrelay and relay systems, all with $L = 20$.

In all simulations, we use binary pulse amplitude modulation (BPAM) for data transmissions and obtain the SNRs (i.e., γ) of the decision variables as follows. First, the signal and noise components of the decision variables for the DCF relay system are exactly generated according to the processing given in (6)–(8), (10), and (11), whereas those for the AF relay system are exactly generated according to the processing given in (37), (38), (40), and (41). Such generation in the DF and DTF cases follows the aforementioned processing, with the modifications described in Sections III-B and IV-B, respectively. Second, calculating the power ratio between the signal and noise components of such a decision variable yields its SNR. This procedure is repeated for several different channel realizations. The histograms of such channel ensembles give a discrete approximation of the pdf of the SNR such that the outage probability, AOF, and BER can be computed. To simplify the simulations, we assume that $N_f = 1$, and hence, $E_f = E_b/2$.

In Figs. 2–9, the numbers in parentheses in the legends represent $M_S, J_R, M_R,$ and J_D , respectively, for the relay systems, and M_S and J_D , respectively, for the nonrelay systems. The

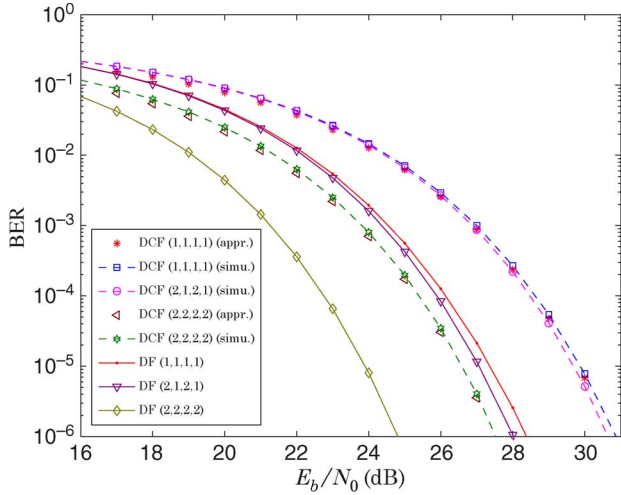


Fig. 4. BERs of the receiver-CSI-assisted relay systems, all with $L = 20$.

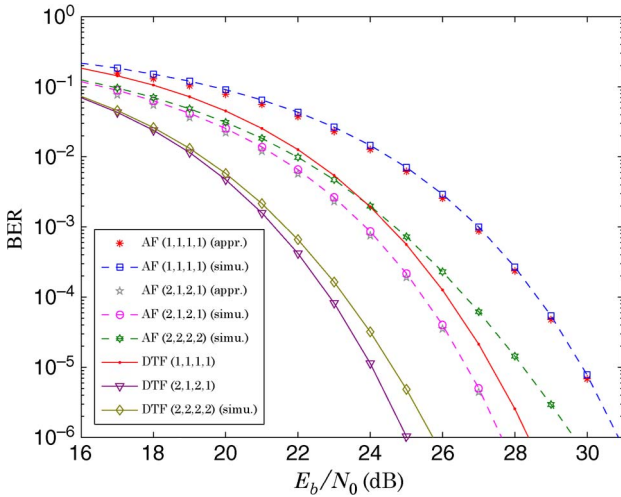


Fig. 5. BERs of the transmitter-CSI-assisted relay systems, all with $L = 20$.

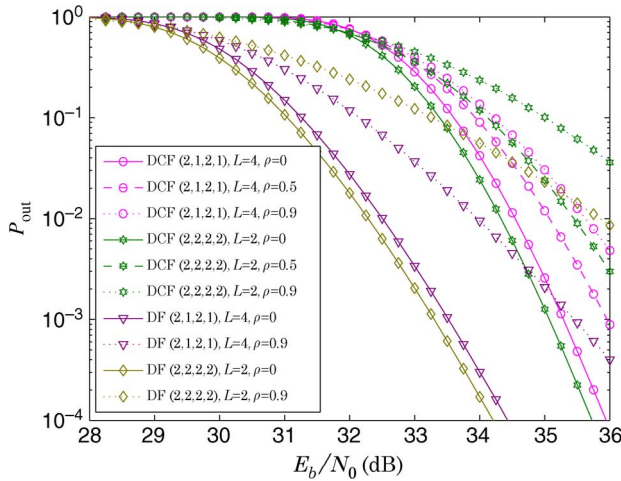


Fig. 6. Effect of the correlation coefficient ρ on the performance of the receiver-CSI-assisted relay systems.

transmit energy per bit in the relay systems is set equal to that in the nonrelay systems, i.e., E_b . In Figs. 2 and 3, and Figs. 6–9, the SNR threshold (γ_{th}) is chosen to be 10 dB.

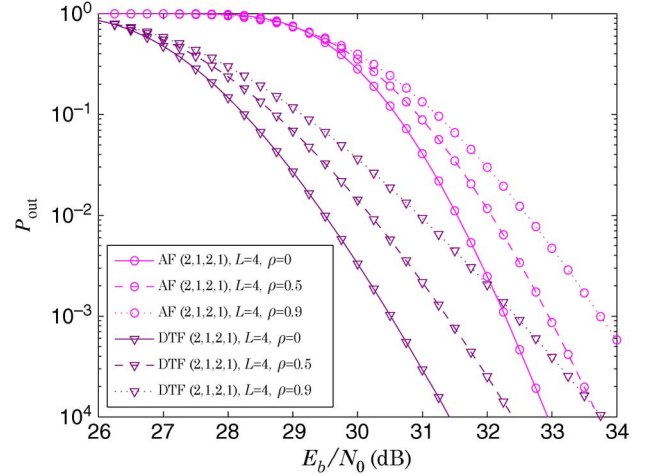


Fig. 7. Effect of the spatial correlation coefficient ρ on the performance of the transmitter-CSI-assisted relay systems.

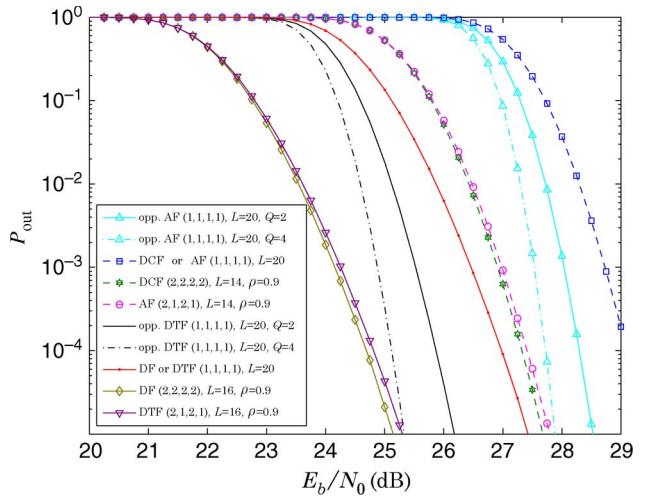


Fig. 8. Comparison of the opportunistic and proposed relay systems.

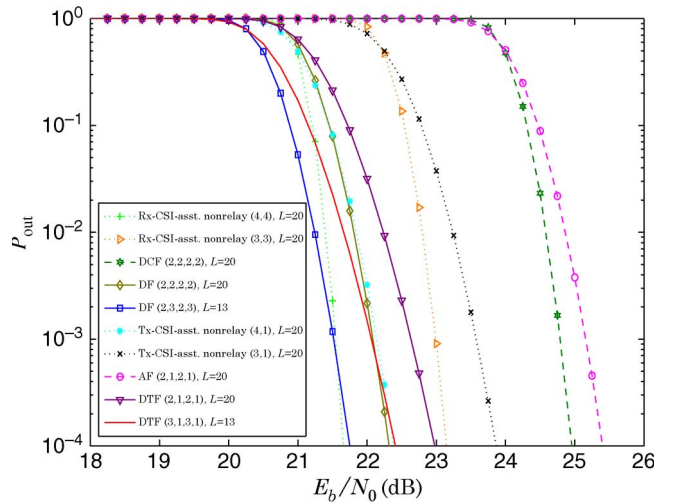


Fig. 9. Comparison of the nonrelay systems with $M_S, J_D > 2$ and the proposed relay systems using fewer transmit and/or fewer receive antennas.

A. Outage, BER, and AOF Performance

Fig. 2 shows the outage probabilities of the receiver-CSI-assisted relay systems [computed with (14) and (25) for the

DCF and DF cases, respectively] and corresponding nonrelay systems (i.e., where the destination knows the channel matrices for the source–destination link, which is denoted by $\{\mathring{\mathbf{H}}_l\}_{l=0}^{L-1}$, all with $L = 20$. The outage results for the nonrelay case are obtained by using

$$P_{\text{out}} = 1 - \sum_{l=0}^{L-1} \sum_{k=1}^{\dot{\mu}} \Delta \left(l, k, \dot{\mu}, \{\dot{\Phi}_q\}_{q=0}^{L-1} \right) \frac{\Gamma \left(k, M_S \gamma_{\text{th}} / (\dot{\gamma} \dot{\Phi}_l) \right)}{(k-1)!} \quad (44)$$

where $\dot{\mu} = M_S J_D \dot{m}$ and $\dot{\Phi}_l = \dot{P} \dot{\Omega}_l / \dot{m}$. We calculate \dot{P} according to [29, eq. (1)]. We set $\dot{m} = m$, $\dot{\Omega}_0 = \Omega_0$, and $\dot{\varpi} = \varpi$. As shown in the figure, deploying multiple antennas improves the outage performance of those systems. Moreover, significant improvement in the outage probabilities of the DCF and DF relay systems is observed when increasing the number of receive antennas, i.e., $J_R = J_D = 2$. This result corresponds to the fact that, in each hop, with the partial CSI at the receiver side, using multiple receive antennas can provide a higher spatial diversity gain compared with using multiple transmit antennas [43]. With the same values of M_S , J_R , M_R , J_D , and L , the DF relay system generally yields a performance gain over its DCF counterpart due to the additional signal processing, i.e., the hard decisions, at the relay.

Fig. 3 shows the outage probabilities of the transmitter-CSI-assisted (i.e., AF and DTF) relay systems and corresponding nonrelay systems (i.e., where the source knows the channel matrices $\{\mathring{\mathbf{H}}_l\}_{l=0}^{L-1}$). The results, except those for the case where $J_R = J_D = 1$, are obtained by simulations and then labeled with “(simu.)” When $J_R = J_D = 1$, the outage probabilities of the AF and DTF relay systems are calculated based on (14) and (25), with the parameter replacement described in Sections IV-A1 and IV-B1, respectively. In the nonrelay case with $J_D = 1$, the outage probability can directly be obtained from (44). It is clear in Fig. 3 that increasing the number of transmit antennas remarkably ameliorates the outage performance, compared with employing a single transmit and receive antenna per hop. This is because the spatial diversity provided by multiple transmit antennas is properly exploited in the transmitter-CSI-assisted systems. On the other hand, increasing the number of receive antennas is not beneficial, because the data transmission structure as represented by (35) [and/or (39)] is simple for the case when $J_R > 1$ (and/or $J_D > 1$).⁶ Advanced space–time coding schemes might improve the efficiency of using multiple receive antennas in this kind of systems.

For the same reason as in the comparison of the DCF and DF relay systems, the outage probabilities of the DTF relay systems are less than their AF counterparts. Comparing Fig. 3 with Fig. 2, one can see that the AF and DCF relay systems, both with (1, 1, 1, 1) and $L = 20$, yield the same

TABLE II
AOFs AT $E_b/N_0 = 25$ dB

System	(M_S, J_R, M_R, J_D)	L	AOF (simu.)	AOF (appr.)
DCF	(1,1,1,1)	20	0.0149	0.0139
DCF	(2,1,2,1)	10	0.0146	0.0131
DCF	(2,2,2,2)	5	0.0142	0.0129
DF	(1,1,1,1)	20	0.0185	0.0193
DF	(2,1,2,1)	10	0.0183	0.0183
DF	(2,2,2,2)	5	0.0177	0.0180
AF	(1,1,1,1)	20	0.0149	0.0139
AF	(2,1,2,1)	10	0.0139	0.0131
DTF	(1,1,1,1)	20	0.0185	0.0193
DTF	(2,1,2,1)	10	0.0173	0.0183

performance. This comes from the fact that, regardless of L , γ for these two systems [i.e., (42) and (12)] are exactly the same when $M_S = J_R = M_R = J_D = 1$. However, for $(M_S, J_R, M_R, J_D) = (2, 1, 2, 1)$ and $L = 20$, the AF relay system yields superior performance. Similar trends can also be observed in the DTF and DF relay systems. Among the considered systems with $L = 20$, the DF relay system with (2, 2, 2, 2) achieves the best performance.

To verify the analytical BER results developed in Sections III-A3, III-B3, IV-A3, and IV-B3, we plot the BER curves of the receiver-CSI-assisted relay systems and those of the transmitter-CSI-assisted relay systems in Figs. 4 and 5, respectively. The analytical high-SNR approximations are labeled with “(appr.)” As shown in both figures, the simulated results closely match the approximate ones, even in the low SNR range, which yields yet less meaningful BERs (e.g., 10^{-1}), and the tightness of the approximations improves as E_b/N_0 increases. Obviously, the results of these two figures support the outage performance comparisons that were presented earlier. Due to their poor performance, the AF and DTF relay systems for the case where $J_R, J_D > 1$ are not discussed in the rest of this paper.

Table II shows the approximate AOFs developed in Sections III-A2, III-B2, IV-A2, and IV-B2, as well as their simulated counterparts, when $E_b/N_0 = 25$ dB and the product of the numbers of transmit antennas, receive antennas, and (pre-)rake fingers is fixed in each hop, in particular $M_S J_R L = M_R J_D L = 20$. We can observe that, for all considered relay systems, the approximate AOFs are in good agreement with the simulated ones. Note that (12) and (42) [or (24) and (43)] are identical when $M_S = J_R = M_R = J_D = 1$. This is the reason why the DCF (or DF) relay system with (1, 1, 1, 1) and $L = 20$ possesses the same approximate and simulated AOFs as its AF (or DTF) counterpart. The results in this table indicate that increasing the number of transmit or receive antennas more efficiently reduces the severity of UWB fading that is experienced by those relay systems than increasing the number of fingers does.

B. Effect of Spatial Correlation

The spatial correlation between the antennas has not been taken into account so far. From a practical point of view, it is important to investigate how such correlation affects

⁶This may be explained, e.g., by considering (42) for the AF relay system. Recall that when $J_R > 1$ (and/or $J_D > 1$), \mathcal{I} (and/or \mathcal{I}') in (42) exists and can take both positive and negative values due to the equiprobable positive or negative polarity of the UWB multipath components, i.e., θ_l included in (1). These negative values can degrade γ in (42), hence, the corresponding outage performance.

the performance of the proposed relay systems. In what follows, we examine this effect on their outage performance. In Appendix A, the detailed calculation of the pdf's and cdf's of \mathcal{E} and \mathcal{E}' in the spatial correlation case is provided. Based on these functions, the outage probabilities of the DCF and DF relay systems are obtained by numerically computing the first line of (14) and the third line of (25), respectively, and the outage probabilities for the AF and DTF cases can similarly be calculated when $J_R = J_D = 1$. Figs. 6 and 7 illustrate the effect of the spatial correlation coefficient ρ on the outage performance of the receiver-CSI-assisted and transmitter-CSI-assisted relay systems, respectively. We set $M_S J_R L = M_R J_D L = 8$ to reduce the simulation time. To make the outage curves readable in Fig. 6, some results at $\rho = 0.5$ are excluded. In both figures, we observe that the outage probabilities of such relay systems increase as the spatial correlation coefficient increases. In particular, the DF and DTF relay systems are slightly more vulnerable to the spatial correlation compared with the DCF and AF ones, respectively. Furthermore, it is apparent in Fig. 6 that, in both the DCF and DF cases, the performance penalty of such correlation becomes more evident when using multiple transmit and receive antennas. Because the spatial correlation in UWB channels mainly depends on antenna spacing [26], the above observations suggest that careful design of this spacing is essential for the UWB MIMO relay systems.

C. Comparison with Opportunistic Relaying

Recently, the opportunistic relaying schemes, in which only the best relay is chosen to be active among all available relays,⁷ have been proposed by Bletsas *et al.* [44] and shown to be outage optimal for a multiple-relay scenario. Note that such outage-optimal schemes resemble our proposed schemes in the sense that only one relay is used to forward data toward the destination. Therefore, it is worthwhile to compare them in terms of their outage probabilities. In the case of opportunistic relaying, we set $J_R = M_R = 1$ for all available relays and $M_S = J_D = 1$, as used in [44]. For convenience of presentation, let $\alpha_{q,l}$ and $\tilde{\alpha}_{q,l}$ be the l th path channel coefficient between the source and q th relay and that between the q th relay and destination, respectively, $\mathcal{Q} = \{1, 2, \dots, Q\}$ be the set of Q available relays, and q^* be the index of the best relay. To conform with the CSI assumption made in [44] but provide a fair comparison with our proposed schemes, we assume that the q th relay knows both $\{\alpha_{q,l}\}_{l=0}^{L-1}$ and $\{\tilde{\alpha}_{q,l}\}_{l=0}^{L-1}$. Under this assumption, two opportunistic relaying schemes, i.e., opportunistic AF and opportunistic DTF, can be considered for UWB data transmissions. In the opportunistic AF scheme, the data transmission from the source to the best relay can be described by (5)–(8) with $M_S = J_R = M_R = J_D = 1$, whereas the one from this relay to the destination can be described by (39)–(41) with these antenna numbers. The description of such data transmissions for the opportunistic DTF scheme can be done

in the same way, except that $\tilde{z}_{R,1}$ in (39) and (40) is substituted by $\hat{b}_{R,1}$, because the best relay makes a hard decision on $z_{R,1}$ in (8) (note that $N_b = 1$ as $M_S = M_R = 1$). Now, the best relay can be represented by its index, i.e.,

$$q^* = \begin{cases} \arg \max_{q \in \mathcal{Q}} \gamma_q, & \text{opportunistic AF} \\ \arg \max_{q \in \mathcal{Q}} [\min(\gamma_{q,1}, \gamma_{q,2})], & \text{opportunistic DTF} \end{cases} \quad (45)$$

where $\gamma_q = \mathcal{E}_q \mathcal{E}'_q \tilde{\gamma}^2 / (\mathcal{E}_q \tilde{\gamma} + \mathcal{E}'_q \tilde{\gamma} + 1)$ is the overall end-to-end SNR per bit, $\gamma_{q,1} = \mathcal{E}_q \tilde{\gamma}$ and $\gamma_{q,2} = \mathcal{E}'_q \tilde{\gamma}$ are the received SNRs per bit for the first and second hops, respectively, $\mathcal{E}_q = \sum_{l=0}^{L-1} \alpha_{q,l}^2$, and $\mathcal{E}'_q = \sum_{l=0}^{L-1} \tilde{\alpha}_{q,l}^2$. Here, we have used the assumption that the equal power allocation between the source and the best relay is adopted. It is not difficult to show that the outage probabilities for both schemes can be written as $P_{\text{out},q^*} = \prod_{q=1}^Q P_{\text{out},q}$, where $P_{\text{out},q}$ in the opportunistic AF and opportunistic DTF cases are expressed as (14) and (25), respectively, both with $M_S = J_R = M_R = J_D = 1$. In Fig. 8, we plot the outage probabilities of the opportunistic relay systems, along with those of our proposed systems. As one can expect, the outage performance of the opportunistic AF and opportunistic DTF systems with $L = 20$ and $Q = 2$ is superior to that of the proposed AF (or DCF) and DTF (or DF) systems with (1, 1, 1, 1) and $L = 20$, respectively. Interestingly, in the outage probability range of interest, the opportunistic AF system with $L = 20$ and $Q = 4$ performs even worse than the proposed DCF (2, 2, 2, 2) and AF (2, 1, 2, 1) systems with $L = 14$ and $\rho = 0.9$. Also, the opportunistic DTF system with $L = 20$ and $Q = 4$ yields poorer outage performance than the proposed DF (2, 2, 2, 2) and DTF (2, 1, 2, 1) systems with $L = 16$ and $\rho = 0.9$. These results imply that the deployment of more transmit and/or receive antennas can be more beneficial compared with inserting additional relays in the SISO single-relay systems (i.e., $M_S = J_R = M_R = J_D = 1$ and $Q = 1$).

D. Further Comparison of the Nonrelay and Proposed Relay Systems

It would be interesting to compare the nonrelay systems with $M_S, J_D > 2$ and the proposed relay systems using fewer transmit and/or fewer receive antennas. To this end, we plot in Fig. 9 the outage curves of these systems. For simplicity, we assume that $M_S = M_R$ and $J_R = J_D$ for the proposed relay systems. In this figure, it is shown that, when M_S, J_D , and L for the nonrelay systems are equal to $M_S + M_R, J_R + J_D$ (except the AF and DTF cases, because $J_D = 1$ in the transmitter-CSI-assisted nonrelay case), and L for their relay counterparts, respectively, the former systems outperform the latter ones. For instance, the receiver-CSI-assisted nonrelay system with (4, 4) and $L = 20$ has better outage performance than the DCF and DF relay systems with (2, 2, 2, 2) and $L = 20$. However, when we deploy more transmit or receive antennas in such relay systems, their superiority over the nonrelay systems can be observed, e.g., the DF (2, 3, 2, 3) and DTF (3, 1, 3, 1) systems with even $L = 13$ exhibit outage performance comparable to the receiver-CSI-assisted nonrelay (4, 4) and transmitter-CSI-assisted nonrelay (4, 1) systems with $L = 20$, respectively. This

⁷We limit our discussion on such schemes to *proactive* opportunistic relaying [44]. *Proactive* means that the relay selection is performed prior to the source transmission.

result also implies that, for UWB relay systems, deploying multiple receive (or transmit) antennas can help reduce the required number of Rake (or pre-Rake) fingers, which is consistent with the nonrelay cases in [43] and [45].

VI. CONCLUSION

In this paper, we have presented the dual-hop UWB MIMO relay systems according to the CSI availability. In particular, the DCF and DF relay systems have been designed with the partial CSI available at the receiver side, whereas the AF and DTF ones have been designed with the partial CSI available at the transmitter side. To study and compare the system performance, we have derived the exact outage probabilities of those systems over a UWB fading channel, except for the AF and DTF cases with $J_R, J_D > 1$. Moreover, we have presented the closed-form approximations for the AOFs and BERs of the systems in the high-SNR regime and shown that these approximations are quite accurate, even in the whole SNR range of interest. The numerical results shed some light on the design of the UWB MIMO relay systems. In addition, the comparison study of our proposed systems and the opportunistic relay systems has been given to assess the effectiveness of the former systems.

APPENDIX A

CDF'S AND PDF'S OF \mathcal{E} AND \mathcal{E}'

Referring back to Section II, let us define $\mu = M_S J_R m$, $\tilde{\mu} = M_R J_D \tilde{m}$, $\Phi_l = P\Omega_l = P\Omega_l/m$, and $\tilde{\Phi}_l = \tilde{P}\tilde{\Omega}_l = \tilde{P}\tilde{\Omega}_l/\tilde{m}$ for ease of exposition. We first consider the case that the channel coefficients $[\mathbf{H}_l]_{ij}$'s are statistically independent and so are $[\mathbf{G}_l]_{ij}$'s. We refer to this case as the *spatial uncorrelation case*. Using (3) and (4), and with the help of [46, eq. (7)], we obtain

$$f_{\mathcal{E}_l}(x; \mu, \Phi_l) = \frac{x^{\mu-1}}{\Phi_l^\mu (\mu-1)!} \exp\left(-\frac{x}{\Phi_l}\right) U(x) \quad (46)$$

$$\begin{aligned} F_{\mathcal{E}_l}(x; \mu, \Phi_l) &= \left[1 - \frac{\Gamma\left(\mu, \frac{x}{\Phi_l}\right)}{(\mu-1)!}\right] U(x) \\ &= \left[1 - \exp\left(-\frac{x}{\Phi_l}\right) \sum_{v=0}^{\mu-1} \frac{1}{v!} \left(\frac{x}{\Phi_l}\right)^v\right] U(x). \end{aligned} \quad (47)$$

Applying [47, Th. 1], the pdf and cdf of \mathcal{E} can be derived, respectively, as

$$f_{\mathcal{E}}(x) = \sum_{l=0}^{L-1} \sum_{k=1}^{\mu} \Delta(l, k, \mu, \{\Phi_q\}_{q=0}^{L-1}) f_{\mathcal{E}_l}(x; k, \Phi_l) \quad (48)$$

$$F_{\mathcal{E}}(x) = \sum_{l=0}^{L-1} \sum_{k=1}^{\mu} \Delta(l, k, \mu, \{\Phi_q\}_{q=0}^{L-1}) F_{\mathcal{E}_l}(x; k, \Phi_l) \quad (49)$$

where

$$\begin{aligned} \Delta(l, k, \mu, \{\Phi_q\}_{q=0}^{L-1}) &= \frac{(-1)^{(L-1)\mu} \Phi_l^k}{[(\mu-1)!]^{L-1} \prod_{q=0}^{L-1} \Phi_q^\mu} \sum_{i_1=k}^{\mu} \sum_{i_2=k}^{i_1} \dots \\ &\sum_{i_{L-2}=k}^{i_{L-3}} \left[\frac{(2\mu - i_1 - 1)!}{(\mu - i_1)!} \left(\frac{1}{\Phi_l} - \frac{1}{\Phi_{0+U(-l)}} \right)^{i_1-2\mu} \right. \\ &\quad \times \frac{(i_{L-2} + \mu - k - 1)!}{(i_{L-2} - k)!} \\ &\quad \times \left(\frac{1}{\Phi_l} - \frac{1}{\Phi_{L-2+U(L-2-l)}} \right)^{k-i_{L-2}-\mu} \\ &\quad \times \prod_{p=1}^{L-3} \frac{(\mu + i_p - i_{p+1} - 1)!}{(i_p - i_{p+1})!} \\ &\quad \left. \times \left(\frac{1}{\Phi_l} - \frac{1}{\Phi_{p+U(p-l)}} \right)^{i_{p+1}-i_p-\mu} \right]. \end{aligned} \quad (50)$$

Following [47, eq. (8)], we can recursively calculate $\Delta(l, k, \mu, \{\Phi_q\}_{q=0}^{L-1})$ as

$$\begin{aligned} \Delta(l, \mu-k, \mu, \{\Phi_q\}_{q=0}^{L-1}) &= \frac{\mu}{k} \sum_{p,q=0, q \neq l}^{L-1} \frac{1}{\Phi_l^{p+1}} \left(\frac{1}{\Phi_l} - \frac{1}{\Phi_q} \right)^{-(p+1)} \\ &\quad \times \Delta(l, \mu-k+p+1, \mu, \{\Phi_q\}_{q=0}^{L-1}) \end{aligned} \quad (51)$$

with $\Delta(l, k, \mu, \{\Phi_q\}_{q=0}^{L-1}) = (1/\prod_{q=0, q \neq l}^{L-1} \Phi_q^\mu) \prod_{p=0, p \neq l}^{L-1} ((1/\Phi_p) - (1/\Phi_l))^{-\mu}$. Similarly, the pdf and cdf of \mathcal{E}' are obtained as (48) and (49), respectively, both with μ being replaced by $\tilde{\mu}$ and Φ_q (and Φ_l) being replaced by $\tilde{\Phi}_q$ (and $\tilde{\Phi}_l$).

Next, we extend the aforementioned derivation to the so-called *spatial correlation case*, where the channel coefficients $[\mathbf{H}_l]_{ij}$'s are statistically correlated and so are $[\mathbf{G}_l]_{ij}$'s. Following the approach outlined in [48], it is straightforward to show that the MGF of \mathcal{E}_l is

$$\mathcal{M}_{\mathcal{E}_l}(s) = [\det(\mathbf{I}_{M_S J_R} - s \Phi_l \mathbf{\Upsilon})]^{-m} \quad (52)$$

where $\mathbf{\Upsilon}$ is the channel correlation matrix. The details regarding the spatial correlation modeling can be found in [25]. For analytical simplicity, it is assumed that the correlation properties at the transmitter side are independent of those at the receiver side [49]. Under this assumption, the correlation matrix is modeled as $\mathbf{\Upsilon} = \mathbf{\Upsilon}_t \otimes \mathbf{\Upsilon}_r$, where $\mathbf{\Upsilon}_t$ and $\mathbf{\Upsilon}_r$ are the $M_S \times M_S$ transmit and $J_R \times J_R$ receive covariance matrices, respectively. Moreover, we assume an exponential correlation model, i.e., deploying an equispaced linear array of antennas at the transmitter side and at the receiver side, and assume the same spatial correlation at both sides. Mathematically, $[\mathbf{\Upsilon}_t]_{pq} = \rho^{|p-q|}$ and $[\mathbf{\Upsilon}_r]_{p'q'} = \rho^{|p'-q'|}$, where ρ is the correlation coefficient between two neighboring antennas, p ,

$q = 1, 2, \dots, M_S$, and $p', q' = 1, 2, \dots, J_R$. Let $\{\lambda_c\}_{c=1}^{N_\lambda}$ be the distinct eigenvalues of \mathbf{Y} , where λ_c has algebraic multiplicity κ_c such that $\sum_{c=1}^{N_\lambda} \kappa_c = M_S J_R$. Hence, the MGF can be expressed as [48]

$$\mathcal{M}_{\mathcal{E}_l}(s) = \prod_{c=1}^{N_\lambda} \frac{1}{(1 - s \Phi_l \lambda_c)^{\kappa_c m}}. \quad (53)$$

Using a partial fraction expansion of the product in (53), we get

$$\mathcal{M}_{\mathcal{E}_l}(s) = \sum_{c=1}^{N_\lambda} \sum_{j=1}^{\kappa_c m} \frac{\epsilon_{c,j}}{(1 - s \Phi_l \lambda_c)^j} \quad (54)$$

where

$$\epsilon_{c,j} = \frac{1}{(\kappa_c m - j)! (-\Phi_l \lambda_c)^{\kappa_c m - j}} \times \left\{ \frac{\partial^{\kappa_c m - j}}{\partial s^{\kappa_c m - j}} \left[\prod_{j'=1, j' \neq c}^{N_\lambda} \frac{1}{(1 - s \Phi_l \lambda_{j'})^{\kappa_{j'} m}} \right] \right\} \Big|_{s = \frac{1}{\Phi_l \lambda_c}}.$$

It is not difficult to verify that $\epsilon_{c,j}$ does not depend on Φ_l , and thereby, the latter can be dropped in the expression of the former. By taking the inverse Laplace transform of $\mathcal{M}_{\mathcal{E}_l}(-s)$ derived from (54), the pdf of \mathcal{E}_l is obtained as follows:

$$\begin{aligned} f_{\mathcal{E}_l}(x) &= \sum_{c=1}^{N_\lambda} \sum_{j=1}^{\kappa_c m} \frac{\epsilon_{c,j} x^{j-1}}{(\Phi_l \lambda_c)^j (j-1)!} \exp\left(-\frac{x}{\Phi_l \lambda_c}\right) U(x) \\ &= \sum_{c=1}^{N_\lambda} \sum_{j=1}^{\kappa_c m} \epsilon_{c,j} f_{\mathcal{X}}(x; j, \Phi_l \lambda_c) \end{aligned} \quad (55)$$

where \mathcal{X} is the Gamma distributed random variable. Thus

$$\begin{aligned} F_{\mathcal{E}_l}(x) &= \sum_{c=1}^{N_\lambda} \sum_{j=1}^{\kappa_c m} \epsilon_{c,j} \left[1 - \frac{\Gamma\left(j, \frac{x}{\Phi_l \lambda_c}\right)}{(j-1)!} \right] U(x) \\ &= \sum_{c=1}^{N_\lambda} \sum_{j=1}^{\kappa_c m} \epsilon_{c,j} F_{\mathcal{X}}(x; j, \Phi_l \lambda_c). \end{aligned} \quad (56)$$

Unlike in the spatial uncorrelation case, the pdf and cdf of \mathcal{E} cannot simply be expressed as the linear summation of (55) and (56), respectively, except for the case where $L = 1$. However, the pdf can numerically be computed as the inverse Laplace transform of $\prod_{l=0}^{L-1} \mathcal{M}_{\mathcal{E}_l}(-s)$, and then, the cdf can readily be obtained. Likewise, the MGF of \mathcal{E}'_l is written as in (52), with M_S, J_R, m, Φ_l , and \mathbf{Y} being replaced by $M_R, J_D, \tilde{m}, \tilde{\Phi}_l$, and $\tilde{\mathbf{Y}} = \tilde{\mathbf{Y}}_t \otimes \tilde{\mathbf{Y}}_r$, respectively. Hence, the pdf and cdf of \mathcal{E}'_l can be derived in the same way as those of \mathcal{E}_l , and the pdf and cdf of \mathcal{E}' can numerically be evaluated.

APPENDIX B PDF OF THE END-TO-END SNR PER BIT FOR THE DCF RELAY SYSTEM

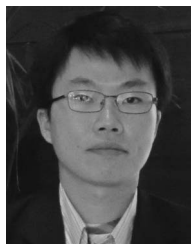
Taking the derivative of (14) with respect to γ_{th} , we obtain the pdf for γ of (12) as

$$\begin{aligned} f_\gamma(x) &= 2 \sum_{l=0}^{L-1} \sum_{k=1}^{\mu} \Delta \sum_{l'=0}^{L-1} \sum_{k'=1}^{\tilde{\mu}} \Delta' \sqrt{\frac{\mathcal{C}_2}{\mathcal{C}_1} \left(1 + \frac{1}{x}\right)} \frac{(\mathcal{C}_1 x / \check{\gamma})^k}{(k-1)!} \\ &\quad \times \exp\left(-\frac{x}{\check{\gamma}} (\mathcal{C}_1 + \mathcal{C}_2)\right) \\ &\quad \times \sum_{j_1=0}^{k'-1} \frac{(\mathcal{C}_2 x / \check{\gamma})^{j_1}}{j_1!} \sum_{j_2=0}^{j_1} \binom{j_1}{j_2} \left[\frac{\mathcal{C}_1}{\mathcal{C}_2} \left(1 + \frac{1}{x}\right) \right]^{\frac{j_2}{2}} \\ &\quad \times \sum_{j_3=0}^{k-1} \binom{k-1}{j_3} \left[\frac{\mathcal{C}_2}{\mathcal{C}_1} \left(1 + \frac{1}{x}\right) \right]^{\frac{j_3}{2}} \\ &\quad \times \left\{ \left[\frac{1}{\check{\gamma}} (\mathcal{C}_1 + \mathcal{C}_2) - \frac{j_1 + k}{x} + \frac{1 + j_2 + j_3}{2x(1+x)} \right] \right. \\ &\quad \times \mathcal{K}_{j_3 - j_2 + 1} \left(\frac{2}{\check{\gamma}} \sqrt{\mathcal{C}_1 \mathcal{C}_2 x (1+x)} \right) \\ &\quad + \frac{1}{2\check{\gamma}} \left(2 + \frac{1}{x} \right) \sqrt{\frac{\mathcal{C}_1 \mathcal{C}_2 x}{1+x}} \\ &\quad \times \left[\mathcal{K}_{j_3 - j_2} \left(\frac{2}{\check{\gamma}} \sqrt{\mathcal{C}_1 \mathcal{C}_2 x (1+x)} \right) \right. \\ &\quad \left. \left. + \mathcal{K}_{j_3 - j_2 + 2} \left(\frac{2}{\check{\gamma}} \sqrt{\mathcal{C}_1 \mathcal{C}_2 x (1+x)} \right) \right] \right\} U(x). \end{aligned} \quad (57)$$

REFERENCES

- [1] M. Z. Win and R. A. Scholtz, "Impulse radio: How it works," *IEEE Commun. Lett.*, vol. 2, no. 2, pp. 36–38, Feb. 1998.
- [2] S. Roy, J. R. Foerster, V. S. Somayazulu, and D. G. Leeper, "Ultra-wideband radio design: The promise of high-speed short-range wireless connectivity," *Proc. IEEE*, vol. 92, no. 2, pp. 295–311, Feb. 2004.
- [3] R. Giuliano and F. Mazzenga, "On the coexistence of power-controlled ultrawide-band systems with UMTS, GPS, DCS1800, and fixed wireless systems," *IEEE Trans. Veh. Technol.*, vol. 54, no. 1, pp. 62–81, Jan. 2005.
- [4] Federal Communications Commission (FCC), "Revision of part 15 of the commission's rules regarding ultra-wideband transmission systems," *First Report and Order*, ET Docket 98-153, FCC 02-48; Adopted: Feb. 2002; Released: Apr. 2002.
- [5] R. Pabst, B. H. Walke, D. C. Schultz, P. Herhold, H. Yanikomeroglu, S. Mukherjee, H. Viswanathan, M. Lott, W. Zirwas, M. Dohler, H. Aghvami, D. D. Falconer, and G. P. Fettweis, "Relay-based deployment concepts for wireless and mobile broadband radio," *IEEE Commun. Mag.*, vol. 42, no. 9, pp. 80–89, Sep. 2004.
- [6] C. Cho, H. Zhang, and M. Nakagawa, "A short delay relay scheme using shared frequency repeater for UWB impulse radio," *IEICE Trans. Fundam. Electron. Commun. Comput. Sci.*, vol. E90-A, no. 7, pp. 1444–1451, Jul. 2007.
- [7] C. Abou-Rjeily, N. Daniele, and J.-C. Belfiore, "On the decode-and-forward cooperative diversity with coherent and noncoherent UWB systems," in *Proc. IEEE ICUWB*, Waltham, MA, Sep. 2006, pp. 435–440.

- [8] C. Abou-Rjeily, N. Daniele, and J.-C. Belfiore, "On the amplify-and-forward cooperative diversity with time-hopping ultra-wideband communications," *IEEE Trans. Commun.*, vol. 56, no. 4, pp. 630–641, Apr. 2008.
- [9] T. Q. S. Quek, M. Z. Win, and M. Chiani, "Distributed diversity in ultrawide bandwidth wireless sensor networks," in *Proc. IEEE VTC*, Stockholm, Sweden, May 2005, vol. 2, pp. 1355–1359.
- [10] S. Zhu and K. K. Leung, "Cooperative orthogonal MIMO-relaying for UWB ad-hoc networks," in *Proc. IEEE GLOBECOM*, Washington, DC, Nov. 2007, pp. 5175–5179.
- [11] K. Maichalernnukul, T. Kaiser, and F. Zheng, "rake fingers versus multiple antennas for UWB relay systems—Which one is better?" in *Proc. IEEE ICUBW*, Hannover, Germany, Sep. 2008, vol. 1, pp. 63–66.
- [12] K. Maichalernnukul, T. Kaiser, and F. Zheng, "Performance investigation of a UWB relay system using multiple relays with multiple antennas in IEEE 802.15.3a channel," in *Proc. IEEE VTC*, Barcelona, Spain, Apr. 2009, pp. 1–6.
- [13] M. O. Hasna and M.-S. Alouini, "End-to-end performance of transmission systems with relays over Rayleigh-fading channels," *IEEE Trans. Wireless Commun.*, vol. 2, no. 6, pp. 1126–1131, Nov. 2003.
- [14] A. Sendonaris, E. Erkip, and B. Aazhang, "User cooperation diversity—Part I: System description," *IEEE Trans. Commun.*, vol. 51, no. 11, pp. 1927–1938, Nov. 2003.
- [15] P. A. Anghel and M. Kaveh, "Exact symbol error probability of a cooperative network in a Rayleigh-fading environment," *IEEE Trans. Wireless Commun.*, vol. 3, no. 5, pp. 1416–1421, Sep. 2004.
- [16] J. N. Laneman, D. N. C. Tse, and G. W. Wornell, "Cooperative diversity in wireless networks: Efficient protocols and outage behavior," *IEEE Trans. Inf. Theory*, vol. 50, no. 12, pp. 3062–3080, Dec. 2004.
- [17] A. Adinoyi and H. Yanikomeroglu, "Cooperative relaying in multi-antenna fixed relay networks," *IEEE Trans. Wireless Commun.*, vol. 6, no. 2, pp. 533–544, Feb. 2007.
- [18] D. Gesbert, M. Shafi, D.-S. Shiu, P. J. Smith, and A. Naguib, "From theory to practice: An overview of MIMO space-time coded wireless systems," *IEEE J. Sel. Areas Commun.*, vol. 21, no. 3, pp. 281–302, Apr. 2003.
- [19] A. J. Paulraj, R. U. Nabar, and D. Gore, *Introduction to Space-Time Wireless Communications*. Cambridge, U.K.: Cambridge Univ. Press, 2003.
- [20] B. Wang, J. Zhang, and A. Høst-Madsen, "On the capacity of MIMO relay channels," *IEEE Trans. Inf. Theory*, vol. 51, no. 1, pp. 29–43, Jan. 2005.
- [21] H. Bolcskei, R. U. Nabar, Ö. Oyman, and A. J. Paulraj, "Capacity scaling laws in MIMO relay networks," *IEEE Trans. Wireless Commun.*, vol. 5, no. 6, pp. 1433–1444, Jun. 2006.
- [22] Ö. Oyman and A. J. Paulraj, "Design and analysis of linear distributed MIMO relay algorithms," *Proc. Inst. Elect. Eng.—Commun.*, vol. 153, no. 4, pp. 565–572, Aug. 2006.
- [23] Y. Fan and J. Thompson, "MIMO configurations for relay channels: Theory and practice," *IEEE Trans. Wireless Commun.*, vol. 6, no. 5, pp. 1774–1786, May 2007.
- [24] I.-H. Lee and D. Kim, "Coverage extension and power allocation in dual-hop space-time transmission with multiple antennas in each node," *IEEE Trans. Veh. Technol.*, vol. 56, no. 6, pp. 3524–3532, Nov. 2007.
- [25] T. Kaiser, F. Zheng, and E. Dimitrov, "An overview of ultra-wideband systems with MIMO," *Proc. IEEE*, vol. 97, no. 2, pp. 285–312, Feb. 2009.
- [26] W. Q. Malik, "Spatial correlation in ultrawideband channels," *IEEE Trans. Wireless Commun.*, vol. 7, no. 2, pp. 604–610, Feb. 2008.
- [27] S. Gradshteyn and I. M. Ryzhik, *Table of Integrals, Series, and Products*, 6th ed. New York: Academic, 2000.
- [28] M. K. Simon and M.-S. Alouini, *Digital Communication over Fading Channels: A Unified Approach to Performance Analysis*. New York: Wiley, 2000.
- [29] D. Cassioli, M. Z. Win, and A. F. Molisch, "The ultra-wide bandwidth indoor channel: From statistical model to simulations," *IEEE J. Sel. Areas Commun.*, vol. 20, no. 6, pp. 1247–1257, Aug. 2002.
- [30] M.-G. Di Benedetto and G. Giancola, *Understanding Ultra Wide Band Radio Fundamentals*. Englewood Cliffs, NJ: Prentice-Hall, 2004, ch. 8.
- [31] H. Liu, R. C. Qiu, and Z. Tian, "Error performance of pulse-based ultrawideband MIMO systems over indoor wireless channels," *IEEE Trans. Wireless Commun.*, vol. 4, no. 6, pp. 2939–2944, Nov. 2005.
- [32] J. Karedal, S. Wyne, P. Almers, F. Tufvesson, and A. F. Molisch, "Statistical analysis of the UWB channel in an industrial environment," in *Proc. IEEE VTC*, Los Angeles, CA, Sep. 2004, pp. 81–85.
- [33] A. F. Molisch, J. R. Foerster, and M. Pendergrass, "Channel models for ultrawideband personal area networks," *IEEE Pers. Commun. Mag.*, vol. 10, no. 6, pp. 14–21, Dec. 2003.
- [34] A. F. Molisch, "Ultrawideband propagation channels—Theory, measurement, and modeling," *IEEE Trans. Veh. Technol.*, vol. 54, no. 5, pp. 1528–1545, Sep. 2005.
- [35] I.-H. Lee and D. Kim, "Decouple-and-forward relaying for dual-hop Alamouti transmissions," *IEEE Commun. Lett.*, vol. 12, no. 2, pp. 97–99, Feb. 2008.
- [36] V. Tarokh, H. Jafarkhani, and A. R. Calderbank, "Space-time block codes from orthogonal designs," *IEEE Trans. Inf. Theory*, vol. 45, no. 5, pp. 1456–1467, Jul. 1999.
- [37] W. P. Siriwongpairat, M. Olfat, and K. J. R. Liu, "Performance analysis and comparison of time-hopping and direct-sequence UWB-MIMO systems," *EURASIP J. Appl. Signal Process.*, vol. 2005, no. 3, pp. 328–345, Jan. 2005.
- [38] D. Cassioli, M. Z. Win, F. Vatalaro, and A. F. Molisch, "Low complexity rake receivers in ultra-wideband channels," *IEEE Trans. Wireless Commun.*, vol. 6, no. 4, pp. 1265–1275, Apr. 2007.
- [39] K. Maichalernnukul, T. Kaiser, and F. Zheng, "Performance of dual-hop MIMO ultra-wideband transmissions: Preliminary results," in *Proc. CISS*, Baltimore, MD, Mar. 2009, pp. 118–123.
- [40] T. Wang, A. Cano, G. B. Giannakis, and J. N. Laneman, "High-performance cooperative demodulation with decode-and-forward relays," *IEEE Trans. Commun.*, vol. 55, no. 7, pp. 1427–1438, Jul. 2007.
- [41] K. Usuda, H. Zhang, and M. Nakagawa, "Pre-Rake performance for pulse-based UWB system in a standardized UWB short-range channel," in *Proc. IEEE WCNC*, Atlanta, GA, Mar. 2004, vol. 2, pp. 920–925.
- [42] S. Imada and T. Ohtsuki, "Pre-Rake diversity combining for UWB systems in IEEE 802.15 UWB multipath channel," in *Proc. Joint UWBST & IWUWBS*, Kyoto, Japan, May 2004, pp. 236–240.
- [43] L.-C. Wang, W.-C. Liu, and K.-J. Shieh, "On the performance of using multiple transmit and receive antennas in pulse-based ultrawideband systems," *IEEE Trans. Wireless Commun.*, vol. 4, no. 6, pp. 2738–2750, Nov. 2005.
- [44] A. Bletsas, H. Shin, and M. Z. Win, "Cooperative communications with outage-optimal opportunistic relaying," *IEEE Trans. Wireless Commun.*, vol. 6, no. 9, pp. 3450–3460, Sep. 2007.
- [45] J. Keignart, C. Abou-Rjeily, C. Delaveaud, and N. Daniele, "UWB SIMO channel measurements and simulations," *IEEE Trans. Microw. Theory Tech.*, vol. 54, no. 4, pp. 1812–1819, Apr. 2006.
- [46] E. Al-Hussaini and A. Al-Bassiouni, "Performance of MRC diversity systems for the detection of signals with Nakagami fading," *IEEE Trans. Commun.*, vol. COM-33, no. 12, pp. 1315–1319, Dec. 1985.
- [47] G. K. Karagiannidis, N. C. Sagias, and T. A. Tsiftsis, "Closed-form statistics for the sum of squared Nakagami-*m* variates and its applications," *IEEE Trans. Commun.*, vol. 54, no. 8, pp. 1353–1359, Aug. 2006.
- [48] M.-S. Alouini, A. Abdi, and M. Kaveh, "Sum of Gamma variates and performance of wireless communication systems over Nakagami-fading channels," *IEEE Trans. Veh. Technol.*, vol. 50, no. 6, pp. 1471–1480, Nov. 2001.
- [49] B. Holter and G. E. Øien, "On the amount of fading in MIMO diversity systems," *IEEE Trans. Wireless Commun.*, vol. 4, no. 5, pp. 2498–2507, Sep. 2005.



Kiattisak Maichalernnukul (S'04) received the B.E. and M.E. degrees in electrical engineering from Chulalongkorn University, Bangkok, Thailand, in 2002 and 2004, respectively. He is currently working toward the Ph.D. degree with the Institute of Communications Technology, Faculty of Electrical Engineering and Computer Science, University of Hannover, Hannover, Germany.

From 2002 to 2004, he was with the Digital Signal Processing Research Laboratory, Center of Excellence in Telecommunication Technology, Chulalongkorn University, as a Graduate Research Assistant. From 2005 to 2006, he was a Research Assistant with the National Electronics and Computer Technology Center, Pathumthani, Thailand. His research interests include communication theory and signal processing for wireless communications. He has made a number of paper contributions and has contributed to two book chapters on ultrawideband topics.



Feng Zheng (SM'06) received the B.Sc. and M.Sc. degrees in electrical engineering from Xidian University, Xi'an, China, in 1984 and 1987, respectively, and the Ph.D. degree in automatic control from the Beijing University of Aeronautics and Astronautics, Beijing, China, in 1993.

Previously, he held an Alexander von Humboldt Research Fellowship with Gerhard Mercator University, Duisburg, Germany, as well as research positions with Tsinghua University, Beijing, the National University of Singapore, Singapore, and the University of Limerick, Limerick, Ireland. From 1995 to 1998, he was with the Center for Space Science and Applied Research, Chinese Academy of Sciences, Beijing, as an Associate Professor. Since July 2007, he has been with the Institute of Communications Technology, Faculty of Electrical Engineering and Computer Science, University of Hannover, Hannover, Germany, as a Wissenschaftlicher Beirat. His research interests include ultrawideband multiple-input–multiple-output (MIMO) wireless communications, signal processing, and systems and control theory. In these areas, he published around 70 refereed journal/conference papers and a book *Ultra Wideband Systems with MIMO* (Wiley, 2010).

Dr. Zheng is a corecipient of several awards, including the National Natural Science Award in 1999 from the Chinese Government, the Science and Technology Achievement Award in 1997 from the State Education Commission of China, and the Best Paper Award in 1994 from the Society of Instrument and Control Engineering (SICE) of Japan at the 33rd SICE Annual Conference in Tokyo, Japan.



Thomas Kaiser (SM'04) received the Diploma degree in electrical engineering from Ruhr University, Bochum, Germany, in 1991 and the Ph.D. (with distinction) and Habilitation degrees in electrical engineering from Gerhard Mercator University, Duisburg, Germany, in 1995 and 2000, respectively.

From 1995 to 1996, he was on research leave with the University of Southern California, Los Angeles, supported by the German Academic Exchange Service. From April 2000 to March 2001, he was the Head of the Department of Communication Systems, Gerhard Mercator University. From April 2001 to March 2002, he was the Head of the Department of Wireless Chips and Systems, Fraunhofer Institute of Microelectronic Circuits and Systems, Duisburg. From April 2002 to July 2006, he was a Coleader of the Smart Antenna Research Team, University of Duisburg-Essen, Duisburg. In Summer 2005, he joined the Smart Antenna Research Group, Stanford University, Stanford, CA. In Winter 2007, he joined the Department of Electrical Engineering, Princeton University, Princeton, NJ, as a Visiting Professor. He is currently the Chair of the Communication Systems Group, Institute of Communications Technology, Faculty of Electrical Engineering and Computer Science, University of Hannover, Hannover, Germany. He is the Founder and the Chief Executive Officer of mimoOn GmbH. He is the author of more than 100 papers in international journals and conference proceedings, and a book *Ultra Wideband Systems with MIMO* (Wiley, 2010). He has been a Guest Editor of several special issues and is a Coeditor of four books on multiantenna and ultrawideband (UWB) systems. He serves on the editorial board of the *EURASIP Journal of Applied Signal Processing*. He is involved in several national and international projects. His research interest focuses on applied signal processing with emphasis on multiantenna systems, particularly its applicability to UWB systems and on implementation issues.

Dr. Kaiser is a Member-at-Large of the Board of Governors of the IEEE Signal Processing Society. He was the Founding Editor-in-Chief of the e-letter of the IEEE Signal Processing Society. He has been the Chair or a Cochair of a number of special sessions on multiantenna implementation issues and is a Member of Technical Program Committee of several conferences. He was the General Chair of the IEEE International Conference on Ultra-Wideband in 2008 and the General Chair of the International Conference on Cognitive Radio Oriented Wireless Networks and Communications in 2009.